11-2020

A NEW GREEN COMPOSITE BASED ON POLYLACTIC ACID MIXED WITH BIOMASS FROM UAE DATE PALM WASTE FOR CUTLERY AND FOOD PACKAGING APPLICATIONS

Noran Hussein Awad Elsayed Mousa

United Arab Emirates University

College of Engineering

Department of Chemical and Petroleum Engineering

A NEW GREEN COMPOSITE BASED ON POLYLACTIC ACID MIXED WITH BIOMASS FROM UAE DATE PALM WASTE FOR CUTLERY AND FOOD PACKAGING APPLICATIONS

Noran Hussein Awad Elsayed Mousa

This thesis is submitted in partial fulfilment of the requirements for the degree of Master of Science in Chemical Engineering

Under the Supervision of Professor Ali Al Marzouqi

November 2020

Declaration of Original Work

I, Noran Hussein Awad Elsayed Mousa, the undersigned, a graduate student at the United Arab Emirates University (UAEU), and the author of this thesis entitled "*A New Green Composite Based on Polylactic Acid Mixed with Biomass from UAE Date Palm Waste for Cutlery and Food Packaging Applications.*", hereby, solemnly declare that this thesis is my own original research work that has been done and prepared by me under the supervision of Professor Ali Al Marzouqi, in the College of Engineering at UAEU. This work has not previously been presented or published or formed the basis for the award of any academic degree, diploma or a similar title at this or any other university. Any materials borrowed from other sources (whether published or unpublished) and relied upon or included in my thesis have been properly cited and acknowledged in accordance with appropriate academic conventions. I further declare that there is no potential conflict of interest with respect to the research, data collection, authorship, presentation and/or publication of this thesis.

Student's Signature: Noran Date: 13th-October-2020

Advisory Committee

1) Advisor: Prof. Ali Al Marzouqi

Title: Professor

Department of Chemical and Petroleum Engineering

College of Engineering

2) Co-advisor: Prof. Basim Abu-Jdayil

Title: Professor

Department of Chemical and Petroleum Engineering

College of Engineering

Approval of the Master Thesis

This Master Thesis is approved by the following Examining Committee Members:

1) Advisor (Committee Chair): Prof. Ali Al Marzouqi

   Title: Professor

   Department of Chemical and Petroleum Engineering

   College of Engineering

   Signature 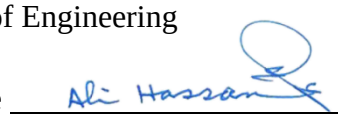 Date 27/12/2020

2) Member: Dr. Muhammad Zafar Iqbal

   Title: Assistant Professor

   Department of Chemical and Petroleum Engineering

   College of Engineering

   Signature  Date 27/12/2020

   For/

3) Member (External Examiner): Dr. Sujan Debnath

   Title: Associate Professor

   Department of Mechanical Engineering

   Institution: Curtin University, Malaysia

   Signature 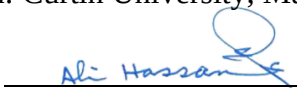 Date 27/12/2020

This Master Thesis is accepted by:

Dean of the College of Engineering: For/ Professor Sabah Alkass

Signature Mohamed AlMarzouqi Date January 03, 2021

Dean of the College of Graduate Studies: Professor Ali Al-Marzouqi

Signature Ali Hassan Date January 03, 2021

Copy ____ of ____

Abstract

Petroleum-based plastic cutlery is widely used and due to their non-biodegradable properties, they cause serious threats to the environment. Therefore, there is a need to fabricate such products from biodegradable material. Date Palm Rachis (DPR) waste was used as a filler in three levels of 30 wt%, 40 wt% and 50 wt% for cost-performance optimization balance and improving the thermal behaviors of the biodegradable Polylactic Acid (PLA). The preparation of biodegradable PLA/date palm waste composites was done using melt mixing extruder at 180°C by varying parameters such as mixing time, the composition of date palm waste biomass, biomass particle size, plasticizers type and plasticizers composition of 1%, 5% and 10% by weight. Biodegradable cutlery along with testing specimens were prepared by compression molding. The produced biodegradable composites were subjected to different characterization and analysis techniques, physical tests, thermal tests, and mechanical tests.

Scanning electron microscope displayed a uniform dispersion of the DPR of 90 μm in the PLA matrix by the addition of 30 wt% biomass and the esterification reaction between –OH of the biomass, the carbonyl (C=O), and the terminal –COOH group in the PLA was observed from Fourier-transform infrared spectroscopy findings. The 30% DPR-PLA composite was considered as the optimum composite because it exhibited lower Melt Flow Index (16 g/10 min) compared to the other two bio-composites, therefore, it will be the best option for processing in large-scale extruders. A slight increase in tensile strength of 30% DPR-PLA composite from 31.82 MPa to 33.20 MPa was noticed by the incorporation of 10 wt% Triethyl citrate (TEC). This research confirmed the superior effect of 10 wt% TEC compared with 10 wt% polybutylene adipate terephthalate (PBAT) in terms of improving the elongation at break of the 30% DPR-PLA composite from 1.8% to 4.20%. However, the water absorption of the 30% DPR-PLA composite for 24 hours was low in saline water (0.25 wt%) and tap water (1.48 wt%) compared with hot water at 50°C (9.34 wt%). On the other hand, the biodegradability tests in outdoor soil showed that the 30% DPR-PLA sample that was placed in the bottom of the watered soil had most color fade off with the highest weight loss of 3.06% after 4 months. This research will have positive consequences on the UAE economy and produce valuable green cutlery

products aligned with both 2021 UAE Vision and 2030 Abu Dhabi Vision in terms of sustainability and innovation in the non-oil sector.

Keywords: Biodegradable, PLA, PBAT, TEC, Date Palm Waste, Cutlery, Green Composites.

Title and Abstract (in Arabic)

مركب أخضر جديد يعتمد على بوليمر عديد حمض اللبنيك الممزوج بالكتلة الحيوية من نفايات النخيل الإماراتية لاستخدامه في أدوات المائدة وحافظات المواد الغذائية

الملخص

تستخدم أدوات المائدة البلاستيكية البترولية على نطاق واسع وبسبب خصائصها غير القابلة للتحلل البيولوجي، فإنها تسبب تهديدات خطيرة على البيئة. لذلك، هناك حاجة لتصنيع مثل هذه المنتجات من مواد قابلة للتحلل. تم استخدام نفايات النخيل (DPR) كمادة حشو في ثلاثة مستويات (٣٠٪ و٤٠٪ و٥٠٪) من حيث الوزن لتحقيق التوازن الأمثل بين التكلفة وتحسين السلوكيات الحرارية لبوليمر عديد حمض اللبنيك (PLA) القابل للتحلل الحيوي. تم تحضير مركبات بوليمر عديد حمض اللبنيك ونفايات نخيل التمر القابلة للتحلل باستخدام آلة الخلط المنصهر عند ١٨٠ درجة مئوية عن طريق تغير معطيات مختلفة مثل وقت الخلط الحراري، وكمية الكتلة الحيوية لنفايات النخيل، وحجم جزيئات الكتلة الحيوية، ونوع المحسنات ومقدار المحسنات بنسبة (١٪ و٥٪ و١٠٪) بالوزن. تم إعداد أدوات المائدة القابلة للتحلل الحيوي والعينات اللازمة للاختبارات المعملية عن طريق قوالب الضغط الحرارية. وقد خضعت هذه المركبات المنتجة القابلة للتحلل الحيوي لمختلف أنواع التحليل، والاختبارات الفيزيائية، والاختبارات الحرارية، والاختبارات الميكانيكية.

قام مجهر الإلكترونات الماسحة بإظهار انتشار منتظم للكتلة الحيوية لنفايات النخيل (٩٠ مايكرومتر) في مصفوفة بوليمر عديد حمض اللبنيك وذلك بإضافة ٣٠ في المئة من الكتلة الحيوية. في حين أن تفاعل الأسترة بين -OH مجموعة الهيدروكسيل في الكتلة الحيوية، مجموعة الكربونيل (C=O)، ومجموعة COOH الطرفية في مصفوفة بوليمر عديد حمض اللبنيك تم ملاحظتها من نتائج تحليل الطيف بأشعة تحت الحمراء "فوربيه". ويعتبر المركب المحتوي على نسبة ٣٠ في المئة من الكتلة الحيوية المركب الأمثل والذي تم اعتماده وتحسينه لأنه يحتوي على أقل مؤشر لتدفق الصهر (١٦ غرام/١٠ دقيقة) مقارنة بالمركبات ذات النسب الأعلى من الكتلة الحيوية لمخلفات النخيل، حيث سيكون أفضل خيار للتصنيع في آلات الخلط المنصهر الكبيرة في المصانع. وقد لوحظ ارتفاع طفيف في قوة الشد لهذا المركب من ٣١.٨٢ ميجا باسكال إلى ٣٣.٢٠ ميجا باسكال عند إضافة ١٠٪ من سترات ثلاثي إيثيل (TEC). تم تأكيد الأثر المتفوق لإضافة١٠٪ من سترات ثلاثي إيثيل (TEC) للمركب الذي تم اعتماده بالمقارنة مع إضافة ١٠٪ بالوزن من البولي بيوتيلين أديباتي تريفثالات

)PBAT(من حيث تحسين عملية الإ طالة عند الكسر من ١.٨٪ إلى ٤.٢٠٪. أما امتصاص المياه لمدة ٢٤ساعة من الغمر لمركب)DPR-PLA٣٠٪(كان منخفضا في المياه المالحة)٠.٢٥٪ (ومياه الصنبور)١.٤٨ ٪(بالمقارنة معالغمر في الماء الساخن)٩.٣٤ ٪(عند ٥٠درجة مئوية. من ناحية أخرى، أظهرت اختبارات التحلل الحيوي في التربة الخارجية أن عينة)-DPR٣٠ PLA٪(التي وُ ضعت في قاع التربة المروية كانت أكثر تلاشيًا في لونها مع أعلى خسارة للوزن بنسبة ٣.٠٦٪ بعد ٤أشهر. سيكون لهذا البحث نتائج إيجابية على اقتصاد دولة الإمارات العربية المتحدة وسينتج م نتجات مائدة خضراء قيمة بما يتوافق مع رؤية الإمارات ٢٠٢١ ورؤية أبو ظبي ٢٠٣٠ من حيث الاستدامة والإبداع في القطاع غير النفطي.

مفاهيم البحث الرئيسية:قابل للتحلل،بوليمر عديد حمض اللبنيك،البولي بيوتيلين أديباتي تريفثالات، سترات ثلاثي إيثيل، نفايات نخيل التمر، أدوات المائدة، المركبات الخضراء.

Acknowledgements

First of all, I would like to express my sincere gratitude to my main supervisor Prof. Ali Al-Marzouqi for his efforts, comments, encouragement, and continuous support. I am especially grateful to my co-supervisor Prof. Basim Abu-Jdayil for his dedicated support, feedback, and guidance. However, many thanks to Emmanuel Galiwango and Sabeera Haris who took part in this research and enabled it to be possible. I would also like to acknowledge the guidance and financial support of Mr. Yousuf-Luiz Caires, the Founder of Palmade, a company established in order to develop a new economy from palm made products to replace single-use plastics in the UAE and the gulf region. Our team meetings and discussions were critical in encouraging me to think outside the box. I would also like to thank my parents; Dr. Hussein Mousa and Dr. Maisa El-Gamal for consistent support and facilitating the conduction of various characterization tests. I would like to thank my research committee, lab technicians and all members of the Department of Chemical Engineering for providing support and considerate guidance. To conclude, thanks for my supporting and loving family and friends for all the unconditional support.

Dedication

To my beloved parents and family

Table of Contents

List of Tables

List of Figures

List of Abbreviations

ASTM	American Society for Testing and Materials
ATBC	Acetyl Tributyl Citrate
°C	Celsius
CH_4	Methane
cm	Centimeter
cm^3	Cubic Centimeter
CNC	Cellulose Nanocrystal
CO_2	Carbon Dioxide
DPR	Date Palm Rachis
DSC	Differential Scanning Calorimeter
FTIR	Fourier Transform Infrared Spectrometry
g	Grams
GPa	Gigapascal
ISO	International Organization for Standardization
J	Joule
kV	Kilovolt
LA	Lactic Acid
MCC	Microcrystalline Cellulose
MFI	Melt Flow Index
min	Minute
mm	Millimeters
mol	Mole
MPa	Megapascal

PBAT	Polybutylene Adipate-co-Terephthalate
PBS	Polybutylene Succinate
PCL	Polycaprolactone
PDLA	Poly D-Lactide
PDLLA	Poly DL-Lactide
PEG	Polyethylene Glycol
PET	Polyethylene Terephthalate
pH	Potential of Hydrogen
PHA	Polyhydroxy Alkanoates
PHB	Polyhydroxy Butyrate
PHBV	Polyhydroxy Butyrate-Valerate
PLA	Polylactic Acid
PLLA	Poly L-Lactide
PP	Polypropylene
PS	Polystyrene
rpm	Revolutions per Minute
SEM	Scanning Electron Microscopy
TEC	Triethyl Citrate
TGA	Thermo-Gravimetric Analysis
μm	Micrometer
€	Euro Currency Sign
$T_{5\%}$	Decomposition Temperature for 5 wt% of a Composite, (^{o}C)
$T_{50\%}$	Decomposition Temperature for 50 wt% of a Composite, (°C)
T_{cc}	Cold Crystallization Temperature, (°C)
T_g	Glass Transition Temperature, (°C)

T_m	Melting Temperature, (°C)
T_{max}	Decomposition Temperature at Maximum Weight Loss, (°C)
wt%	Weight Percentage
ΔH_c	Crystallization Enthalpy, (J/g)
ΔH_m	Melting Enthalpy, (J/g)

Chapter 1: Introduction

1.1 Overview and research objectives

Most petroleum-based plastics are non-biodegradable and commonly used in almost every field. They are manufactured as non-biodegradable based on a business point of view to improve the quality of plastics by giving them long-lasting effects, more temperature resistant, and more durable even after use. Most of the inorganic wastes can be considered as non-biodegradable waste. A non-biodegradable waste cannot be easily handled as it cannot be dissolved by natural agents or decomposed. Simply they cannot be broken down by natural organisms, so they act as a source of pollution in landfills and oceans by remaining on earth for thousands of years without any degradation. They are the main causes of air, water, and soil pollution and diseases like cancer. These plastics need to be replaced as soon as possible as they are not eco-friendly. Scientists have carried many ideas such as biodegradable plastics or incorporated certain biodegradable components with plastics and made them easily degradable.

The awareness and interest of the development and study of biodegradable polymers that could replace petroleum-based plastics in all applications are rising to reduce the environmental impacts of non-biodegradable polymers or composites and decrease dependence on petroleum products. Polylactic Acid (PLA) is a good example of biodegradable polymer with high mechanical properties and biocompatibility. PLA is produced by fermentation from agricultural products like corn, sugar cane, potato, and rice. Some disadvantages of using PLA without filler could be the high cost of production, low thermal stability, and brittleness. To optimize the cost-performance balance and enhance mechanical and thermal properties; biodegradable fillers like

lignocellulosic biomass could be a good solution instead of synthetic fibers like glass. The advantages of biodegradable natural fillers are mainly their abundance, high stiffness, non-abrasiveness to the processing equipment, low density, and low cost [1]. Another example of a biodegradable polymer is starch. Starch films are attractive for food packaging applications and have the ability to degrade into harmless products by the microorganisms in the soil [2].

The UAE produces 500,000 tons of date palm waste every year [3]. These are disposed of in landfills or burned in farms causing environmental pollution which can lead to global warming and its consequences due to the huge amounts of CO_2 produced from burning date palm waste. Date palm biomass is a lignocellulosic material made mainly from cellulose, hemicellulose, and lignin. However, cellulose is the most important skeletal component of wood carbohydrate, the polysaccharide cellulose is an almost inexhaustible polymeric raw material with attractive properties and structure. Cellulose can be extracted from different parts of date palm waste like leaflet, rachis, and fiber as displayed in Figure 1. Hence, date palm waste biomass can be used to reinforce different polymeric matrices like starch, Polylactic Acid, Polyvinyl Alcohol, and other polymers [4].

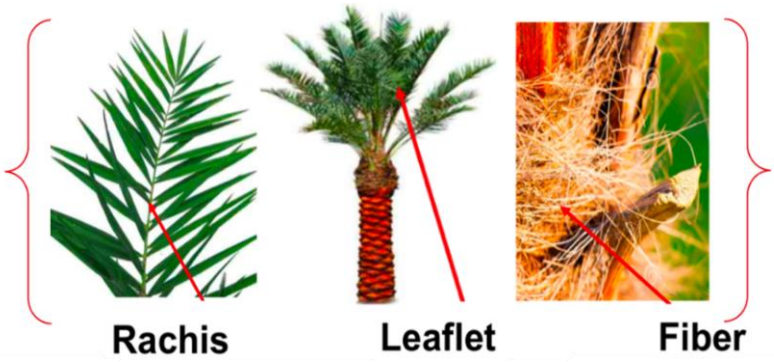

Figure 1: Different parts of date palm waste.

The goal of this research was to develop a new green composite suitable for cutlery and food packaging applications by replacing petroleum-based materials used in single-use plastics with a sustainable biodegradable waste material from UAE Date Palm Rachis (DPR) and Polylactic Acid (PLA) as shown in Figure 2. PLA was considered to be a suitable polymer that would be compatible with conventional biodegradable polymers to be used in the preparation of the date palm biomass-polymer composite. The objectives of this study are the following:

1. Prepare composites of whole DPR with PLA in an extruder.
2. Prepare composites of cellulose extracted from DPR with PLA and to compare with composites using the whole DPR as a filler.
3. Characterize the fabricated new biodegradable composites for their physical, thermal, and mechanical properties to be compared with the specifications of plastic cutlery available in the market.
4. Investigate the effects of parameters such as the composition and particle size of biomass or cellulose, melting temperature, melt mixing time, and plasticizer type and amount on the physicochemical properties of the prepared composites.

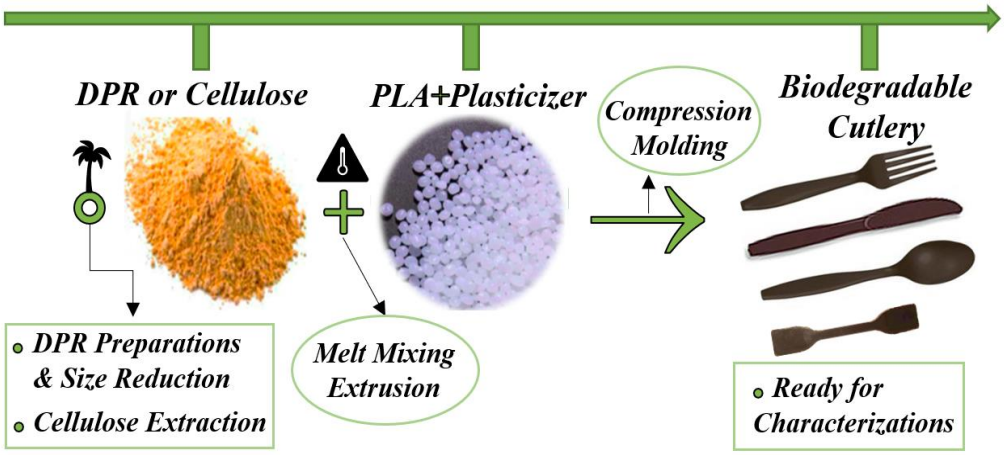

Figure 2: The fabrication methodology for the biodegradable DPR-PLA cutlery.

This work utilizes UAE date palm waste for the production and preparation of green biodegradable composites intended for cutlery and packaging applications with competitive properties. The possibility of utilizing the whole DPR waste without extraction as a filler to produce DPR-PLA composite has not been studied before. This research was focused on the effect of the addition of biomass (30 wt%, 40 wt%, and 50 wt%) to the PLA matrix on the properties of the resulting composite material including phase adhesion, degradation temperature, glass transition temperature, and Melt Flow Index. Effect of a maximum of 10 wt% of two food grade plasticizers (TEC and PBAT) to enhance the mechanical properties of the DPR-PLA composite material was studied for the first time. Also, water absorption and biodegradation of the optimum DPR-PLA composites under real local soil conditions were investigated.

1.2 Petroleum-based plastic and corresponding waste problems

The plastic term came from a Greek word called “plastikos” and it means the ability to maintain its shape to be used in different applications. Plastics are long chains of polymer molecules that are extracted from petroleum, natural gas, and coal. The world plastic production has risen from 2 million tons per year in 1950 to 381 million tons per year in 2015 [5]. The two main types of plastics are thermoset and thermoplastic. Thermoset plastic cannot melt once it is formed because they are nonlinear and cross-linked polymers. The most produced and consumed plastics are thermoplastics. Thermoplastics are linear polymers with the ability to re-melt and reshape several times [6]. Figure 3 shows the structures of a linear, branch, and cross-linked polymers [7]. The main advantages of plastics are the low manufacturing cost, good mechanical performance, and durability [8].

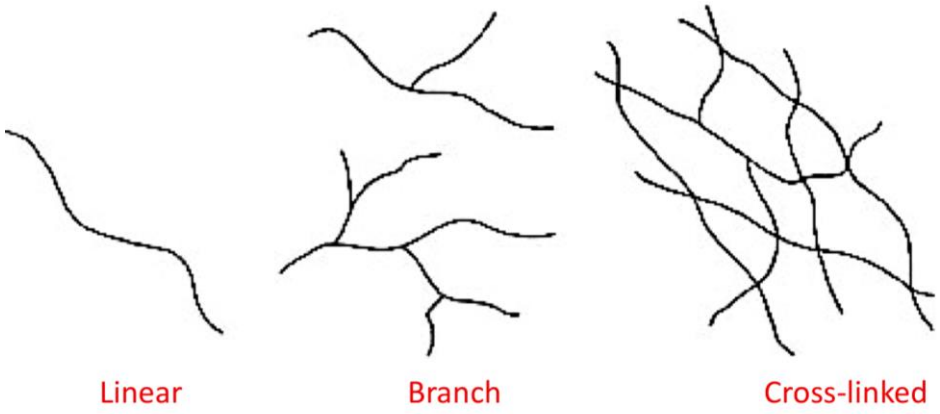

Figure 3: Representative skeletal structures of a linear, branch, and cross-linked polymers [7].

Petrochemical-based plastics such as Polypropylene (PP), Polyethylene Terephthalate (PET) and Polystyrene (PS) have been used as packaging and food contact materials because they are largely available at low cost and good performance. However, plastic wastes and their corresponding microplastic contaminants pollute the world's oceans by 13 million metric tons of plastic per year. They will cause suffocation, starvation, and drowning for seabirds, marine mammals, fish, and sea turtles. They are killed by ingesting plastic debris as shown in Figure 4 [9]. Many toxic chemicals such as dioxins are released from plastics. They cause cancer, chronic respiratory disorders, neurological damage, and other health problems [10]. Plastics are non-biodegradable, but they undergo the process of photo-oxidation or UV radiation or even sunlight [11]. This process will release toxic gases, dioxins, polychlorinated biphenyls, and furans [12].

Figure 4: A dead albatross due to ingesting plastic debris in the Pacific Ocean [9].

1.3 Biodegradable polymers as an alternative solution

Recently, the accumulation of trillions of plastic wastes in landfills and oceans has increased the environmental and health concerns. These concerns strongly shift the researchers' attention to the demands for developing biodegradable and renewable materials in various applications such as medical and food packaging. The application field of food packaging includes drinking cups, stirrers, plates, cutlery, straws, and food containers. These items must be fabricated to be in contact with aqueous, fatty, and acidic foods bellow room temperature or as high as 60°C [13]. A balance between food protection and other considerations such as good mechanical performance, cost and energy is highly recommended [14]. Natureworks LLC., the main resin producer, recorded that bioplastics synthesis produces 60 wt% fewer greenhouse gases when compared to petroleum-based polymers production [15].

1.3.1 Biodegradability concept

The biodegradability concept is directly related to the chemical structure of the polymers despite their origin. Biopolymers fabricated from renewable resources are

biodegradable and compostable and can act as a soil fertilizer. On the other hand, plastics from renewable resources might not be biodegradable or compostable. Many bioplastics are fabricated from non-renewable materials as illustrated in Table 1. The degradation in landfills occurs via microorganisms such as fungi and bacteria by an enzymatic process. But non-enzymatic degradation could break the polymer chains by chemical hydrolysis. The end products for degradation are CO_2, water, CH_4, biomass, and other natural substances. The recyclable biological process of biodegradation is shown in Figure 5. For biopolymers, the plants are grown then polymerization will take place. The final products will be used by consumers then dumped in landfills to be composed to end products that will maintain sustainability. The degradation rate will rely on humidity, temperature (50–70°C), and type and number of microbes. In general, industrial composting is much faster (around 6 to 12 weeks) compared to the slow outdoor biodegradation [16].

Table 1: Classifications of polymers based on resource types and end of life option [17].

Resource Basis of a Material	End of Life Option: Non-Biodegradable Plastics	End of Life Option: Biodegradable Plastics
Bio-Based Resources	Bio-Based PE, PET, PA	Starch Blends, PLA,PHA
Fossil Resources	Conventional PE, PET, PA	Aliphatic-Aromatic Polyesters

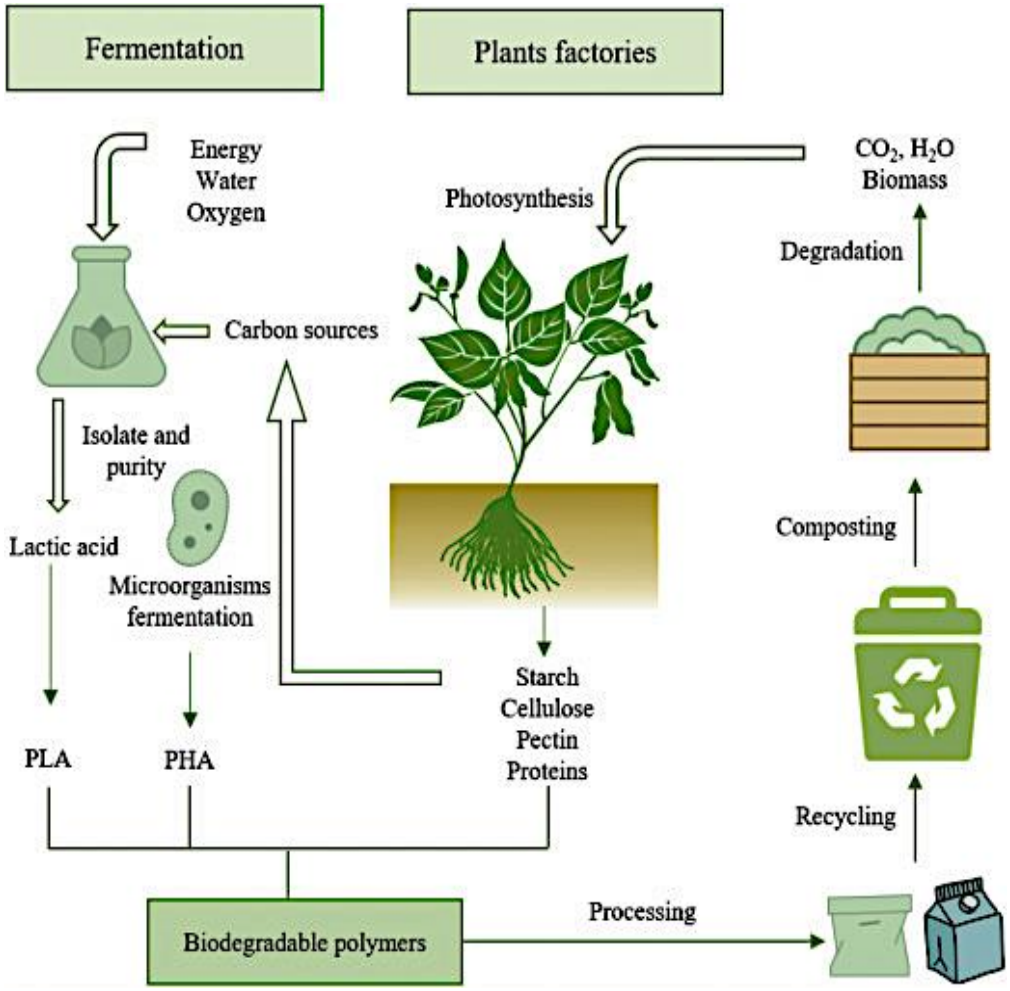

Figure 5: Cyclic biological process of biodegradability [18].

1.3.2 Durability and cost

Petroleum-based polymers are durable compared to biodegradable polymers since petroleum-based polymers start to decompose after 500 years. Some biodegradable polymers such as PLA can degrade after 10 to 20 years in indoor conditions. However, it is totally biodegradable at industrial compostable conditions in a much shorter time. The price of bio-based and biodegradable polymers is high on a weight basis compared to petroleum-based polymers because of the high density of bio-based polymers. There are some exceptions for biodegradable polymers such as PLA. The high stiffness of PLA compared to PS will help to reduce its thickness and

therefore its cost. Unfortunately, petroleum-based polymers' prices are not stable due to the fluctuations in oil prices. In this case, the price of biopolymers is more stable and may drop due to the effect of the economy of large scale and conversion [19].

1.3.3 Biodegradable polymers classification

The biodegradable polymers are classified according to their sources to biopolymers from renewable resources and polymers from petrochemical resources such as Polycaprolactone (PCL) as shown in Figure 6. The biopolymers from renewable resources are subclassified according to their source and synthesis process. The first category is directly from biomass such as polysaccharides and proteins, the second category consists of synthetic biopolymers from biomass like Polylactic Acid (PLA), and the last category contains those obtained by microorganisms by microbial fermentation like Polyhydroxy Alkanoates (PHA). PLA and starch-based polymers are common bio-based polymers to be used in food packaging applications. Figure 7 presents the structure of common biodegradable polymers. The characteristics of selected biodegradable polymers will be introduced as the following.

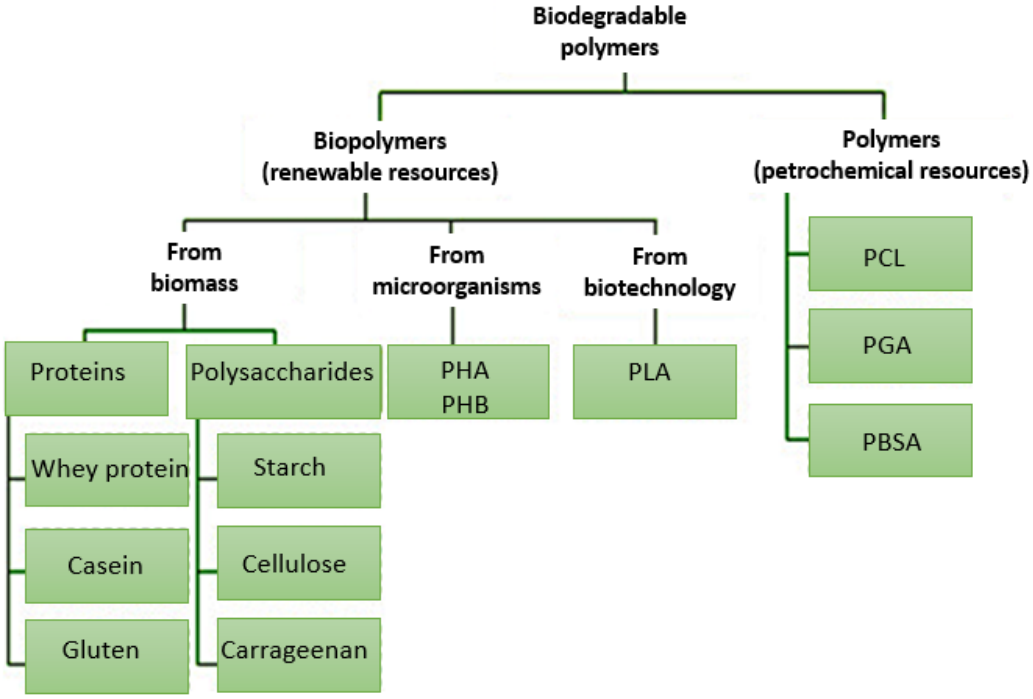

Figure 6: Representative biodegradable polymers based on two resources [12].

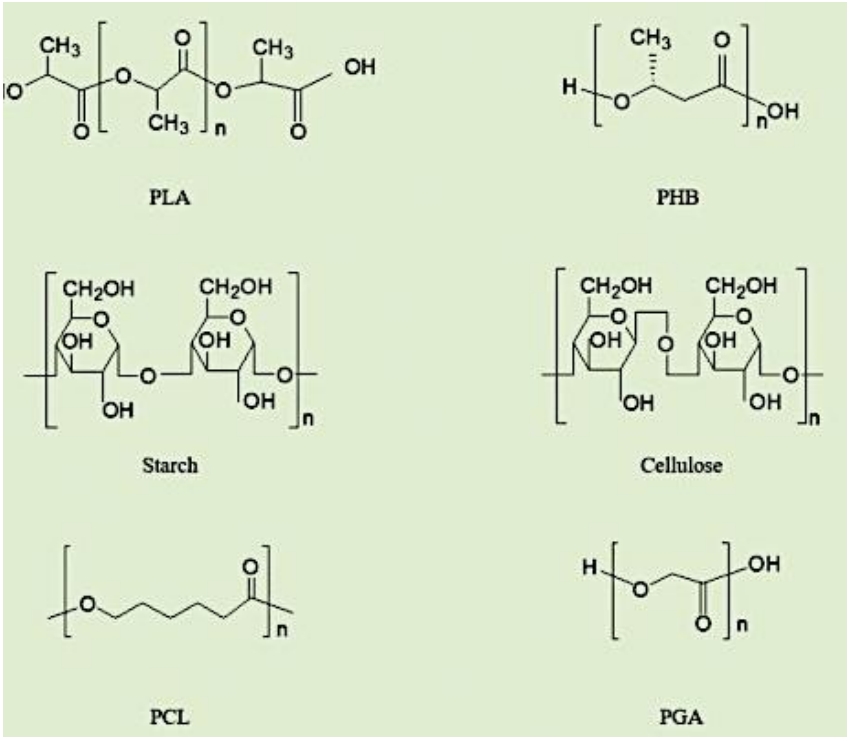

Figure 7: The structure of common biodegradable polymers [18].

Starch is classified as one of the most abundant polysaccharides biopolymer from plants [20]. Amylopectin and amylose are the main glucose constituents of native starch. Starch as a biodegradable polymer can be processed in large quantities to form films with low oxygen permeability due to its low cost. Starch can be used in plastic bags and food packaging [21]. Unfortunately, starch as a biopolymer has many limitations regarding processing due to its brittleness and hydrophilic characteristics. To resolve these drawbacks and improve its flexibility, starch needs to be converted into thermoplastic starch (TPS) by extrusion shearing processes [22, 23].

Cellulose is another highly polar biopolymer composed of glucose units based on renewable polysaccharides in plants. Cellulose has stronger mechanical properties and hydrolysis resistance when compared to starch. It forms stronger hydrogen bonds due to its mixed morphology and different polymer chain configuration than those in starch. On the other hand, cellulose extraction is more expensive than starch, especially due to the expensive pre-treatment stages in the case of cellulose [24]. The resultant pure cellulose could be further chemically modified to produce cellulose derivatives with enhanced properties. However, these modifications are costly [25, 26]. Furthermore, films produced from uncoated cellulose are highly permeable to water vapor and suitable barriers to bacteria, aromas, and flavor [26].

PLA is a biodegradable readily available and cheap polyester produced from Lactic Acid by the fermentation of crops like corn. PLA exhibits accepted properties for packaging and applications that involve food contact. Transparency, biocompatibility, processability, and stiffness are the main reason to use PLA in such applications. Table 2 shows different examples of biodegradable polymers and petroleum-based polymers with their characteristics and possible natural filler reinforcement. PLA shows better thermal processability when compared with other

biodegradable biopolymers such as Polycaprolactone (PCL), Polyhydroxy Alkanoates (PHA), and Polyethylene Glycol (PEG). This special characteristic allows the PLA to be processed in wide methods such as melt mixing extruder, injection molding, compression molding, fiber spinning, blow filming, thermoforming, and cast film [27]. However, PLA is brittle with less than 10% elongation at break which means it will not be suitable for applications that require plastic deformation at high levels of stress. To address this limitation, PLA needs to be blended with other biopolymers or natural fillers that have specific properties to decrease its brittleness and enhance its mechanical properties.

Polyhydroxy Alkanoates (PHA) are mostly thermoplastic biodegradable polymers obtained naturally by bacterial fermentation of lipids or sugars. The melting point of these polymers ranges from 40°C to 180°C according to the used monomer and they are excellent for packaging films [28] . Polyhydroxy Butyrate (PHB) is the most well-known type of these polymers. PHB has similar properties to Polypropylene (PP) but more brittle and stiffer. Polyhydroxy Butyrate-Valerate (PHBV) is less brittle and can be used as a packaging material that can degrade within 6 weeks in industrial composting conditions, however, it is costly. PHB is a good additive for PLA to improve its mechanical properties. The MARGIN project in Poland allowed the production of thermoformed biodegradable food packaging from PLA with an atactic PHB additive.

Table 2: Biodegradable polymers and petroleum-based polymers with their characteristics and possible natural fillers reinforcement.

	Biodegradable Polymers			Petroleum-based Polymers		
	(Food Grade approved by FDA)					
	PLA (2003D)	PCL	PHB	PET	PS	PP
Application [a]	-Packaging and paper coatings. -Sustained release systems for pesticides. -Mulch films, and compost bags.	-Long-term items; mulch and other agricultural films. -Containers; slow-release systems for drugs.	-Bottles, bags, and wrapping film. -Controlled drug release carriers.	-Carbonated soft drink bottles. -Processed meat Packages. -Peanut butter jars. -Sleeping bags.	-Disposable cups. -Packaging materials. -Laboratory ware. -Electronic uses.	-Bottle caps. -Drinking straws. -Medicine bottles. -Car seats and batteries. -Carpet backings.
Cost (€/kg) [b]	0-2	-	4-12.02	1.71-1.8	2-2.4	1.71-2
Melting point (°C) [c]	120-170	60-65	180	245-265	-	160-208
Glass Transition (°C) [c]	55-56	–60	55	69-115	97	–18
Onset Thermal Degradation	278.5 [c]	234 [d]	272.7 [e]	401 [f]	369 [f]	336-366 [c]
MFI (g/10 min)	6 [g]	14.5 [h]	21.2 [i]	28.94 [j]	11.57 [k]	5.9 [l]
Impact Strength (J/cm) [c]	0.20	1.20	0.22	-	19.7	0.3-2
Tensile Strength (MPa)	51.38±1.19 [m]	40.60±3.06 [m]	36.4±2.8 [n]	59.6±2.9 [o]	25-69 [p]	26-41.4 [p]

a: [29], b: [30], c: [31], d: [32], e: [33], f: [34], g: [35], h: [36], i: [37], j: [38], k: [39], l: [40], m: [41], n: [42], o: [43], p: [44]

Table 2: Biodegradable polymers and petroleum-based polymers with their characteristics and possible natural fillers reinforcement (Cont.).

	Biodegradable Polymers			Petroleum-based Polymers		
	(Food grade polymers that approved by FDA)					
	PLA (2003D)	PCL	PHB	PET	PS	PP
Modulus (GPa)	1.09±0.03719 [m]	0.22±0.0052 [m]	2.99±0.209 [n]	2.467±1.99 [o]	4-5 [p]	0.95-1.77 [p]
Elongation (%)	6.64±0.46 [m]	1996±221 [m]	2.1±0.3 [n]	5.2±1.6 [o]	1-2.5 [p]	15-700 [p]
Water Absorption after 24 hours (wt%)	0.125 [q]	0.01 [r]	0.3 [s]	0.5 [t]	0.03-0.10 [p]	0.01-0.02 [p]
Reinforcement Effects	Incorporation of 5 wt% MCC enhanced the thermal stability but reduced the elongation and tensile strength of PLA matrix. [u]	Addition of 50 wt% cocoa shell waste to 3D printed PCL showed a good adhesion and fine resolution for biomedical applications. [v]	Addition of up to 5 wt% CNC improved gas barrier and migration properties of PHB. [w]	Incorporation of up to 20 wt% treated moringa oleifera fiber increased the mechanical properties of PET. [x]	Agave leaves (2 wt%) reinforced Polystyrene showed good interfacial adhesion. [y]	Addition of 30 wt% hemp fiber increased the ultimate tensile strength and Young's modulus by more than 50% and 143%, respectively. [z]

m: [41], n: [42], o: [43], p: [44], q: [45], r: [46], s: [47], t: [48], u: [49], v: [50], w: [51], x: [52], y: [53], z: [54]

Polycaprolactone (PCL) is a biodegradable polymer obtained from petrochemical resources by the polymerization of ε-caprolactone. PCL is a quite expensive thermoplastic polyester. It has a low melting point (60–65°C) [25], and good thermal processability. Due to its low melting point, PCL alone is not a good option for food packaging applications. PCL is mostly blended with other polymers such as cellulose acetate butyrate and cellulose propionate to enhance adhesion and stress crack resistance [55].

1.3.4 Main processing of biodegradable polymers

Melt mixing extrusion is a large capacity manufacturing process in which one type or more of raw granular polymer is melted and mixed to form a continuous homogenous profile. The polymer granular pellets and other additives are gravity-fed through a hopper on the top into the barrel of the extruder as shown in Figure 8. Additives, such as antioxidant, plasticizer, compatibilizer, and colorants could be in liquid or solid pellets form. These additives are mixed either in separate mixer prior to arriving at the hopper or directly at the hopper. The mixture of polymer pellets and other additives is pushed through the barrel to be melted and mixed taking into consideration to avoid overheating and polymer degradation. Then the molten plastic enters the die which defines the final product's continuous profile shape. Finally, the product is cooled by air or pulling the extruded part through a water bath.

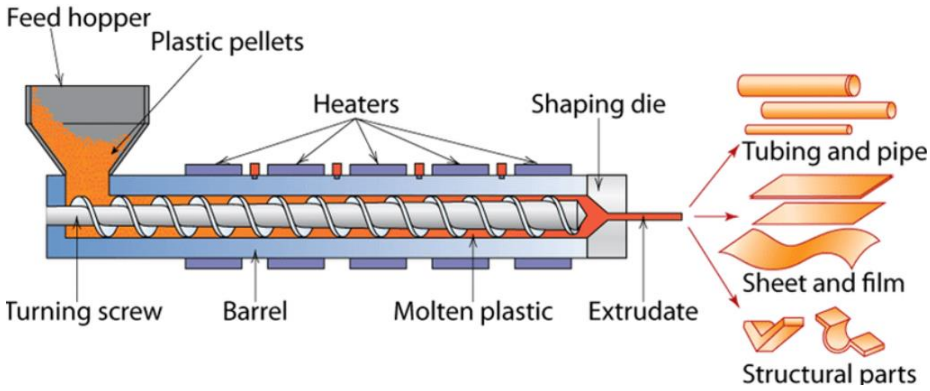

Figure 8: Extrusion machine layout [56].

Injection molding is a common industrial process in which the plastic is melt mixed then forced into a mold of specific cavities by a reciprocating screw. The homogenous molten plastic is injected at high-pressure to fill the closed mold cavity of a certain shape. The mold plates must be closed by hydraulic or mechanical clamping force during the injection. This force should oppose the separating force of the injection of the molten plastic. The mold is cooled to allow the solidification of the final plastic product. The two plates of the mold are separated to allow the collection of the final product. Figure 9 presents the layout of the injection molding machine.

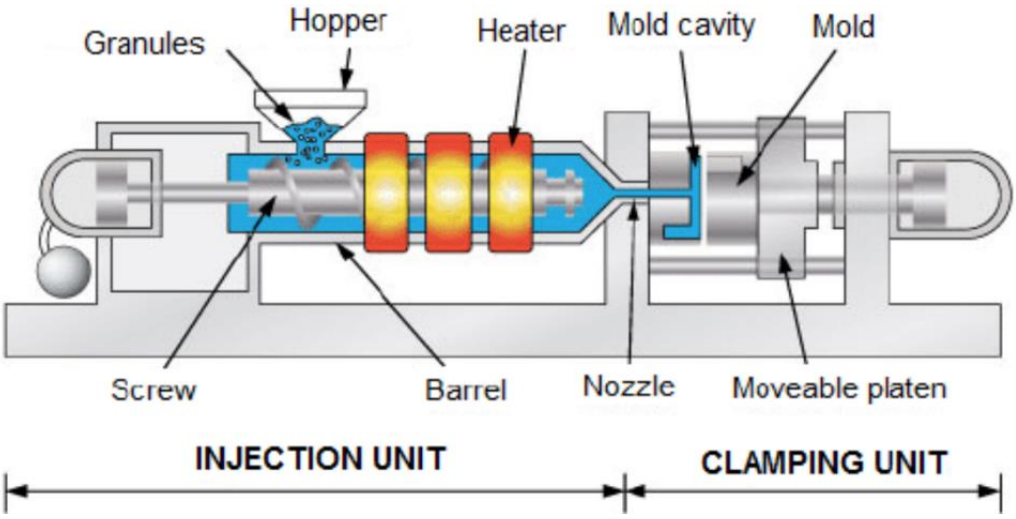

Figure 9: Injection molding machine layout [57].

1.4 Natural fibers

Natural fibers are usually abundant throughout the world as waste material. The increase in environmental concerns directed the awareness of the use of biodegradable environmentally friendly materials and lignocellulosic natural fibers. Natural fibers are usually classified with respect to their origins: animal, vegetable (or lignocellulosic), or mineral as shown in Figure 10. The date palm, oil palm, hemp, sisal, kenaf, pineapple leaf, and jute are the most common lignocellulosic natural fibers [58]. Natural fiber may be used as an alternative filler instead of synthetic fiber to reinforce thermoplastic and thermoset polymer composites to enhance their thermal, physical, and mechanical properties. Some advantages of natural fibers, when compared to synthetic fibers, are fast biodegradation, low cost, low density, low energy consumption, and non-abrasive characteristic [59, 60]. The surface modification of natural fiber is mandatory to clean and purify the fiber from impurities or undesired components for better adhesion between the polymer and the fiber [61].

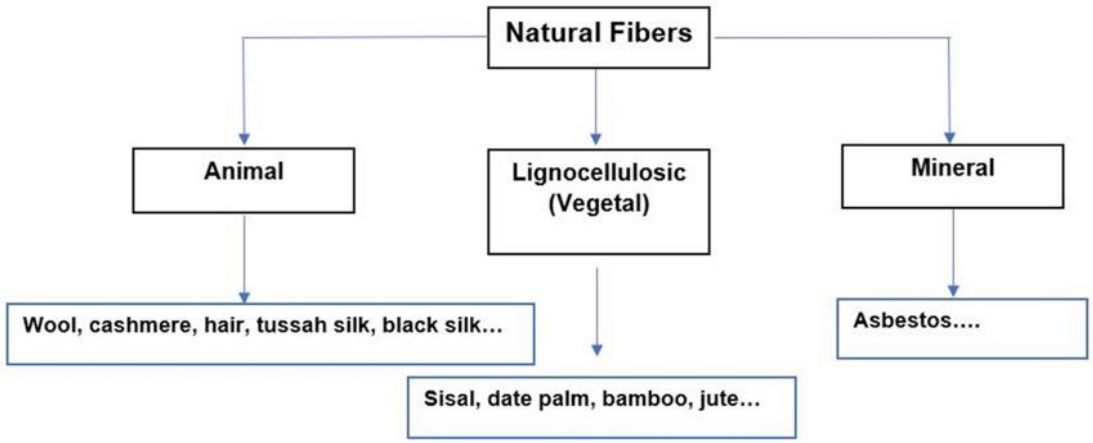

Figure 10: Natural fibers according to their origins [62].

1.4.1 Chemical composition of lignocellulosic fibers

Cellulose, hemicellulose, and lignin as presented in Figure 11 are the major constituents of lignocellulosic fibers with different percentages depending on the fiber age, climatic conditions, humidity, and origin [63]. Cellulose is the major component in lignocellulosic fibers with a weight percent varying from 40% to 60% as shown in Table 3. Hemicelluloses are the second major constituent with a weight percent varying from 20% to 40%. However, lignin comes in third place from 10 to 25% by weight percent [64, 65]. Other components such as waxes, inorganic salts, proteins, and pectin go from 4 to 10 % weight percent and they are characterized by their ash content [61]. Lignocellulosic fibers are hydrophilic due to the hydroxyl groups presented on the surface of the fibers, thus resulting in poor adhesion between the fiber and the polymer matrix and poor mechanical performance. This limitation can be addressed during the fiber processing prior to reinforcement by removing hemicellulose through hydrothermal treatment and increasing cellulose crystallinity [66].

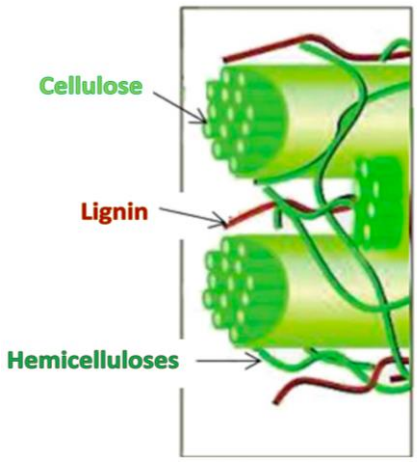

Figure 11: The main structure of the lignocellulosic fiber [67].

Table 3: The chemical composition and mechanical properties of various types of lignocellulosic fibers [59].

Lignocellulosic fibers	Date palm	Ramie	Sisal	Hemp	Jute
Cellulose (%)	32–35.8	68–91	47–78	57–77	64.4
Hemicelluloses (%)	24.4–28.1	5–16.7	10–24	14–22	12
Lignin (%)	26.7–28.7	0.6–0.7	7–11	3.7–13	11.8
Other components (%)	2–7	–	1–10	–	5–11
Density (g/cm^3)	1.4	1.5	1.5	1.4	1.4
Tensile strength (MPa)	150–230	500	511–635	550–900	400–800
Young modulus (GPa)	2–7.5	44	9.4–22	70	10–30
Elongation (%)	5–10	3.6–3.8	2–2.5	1.6	1.8

1.4.2 Mechanical properties and thermal stability of natural fibers

The mechanical properties of the natural fiber reinforced polymer composites generally depend on the mechanical properties of the fibers such as fiber density and microfibril angle. For example, fibers with low density show higher stiffness and strength when compared to high-density fibers [68]. The tensile strength of fibers is a main mechanical test in which a stretching force is applied, and the maximum tensile stress amount is recorded before breaking. A study on different fibers revealed that palm fiber had the highest tensile strength of 160 MP compared with all the studied fibers [69]. The chemical, physical and mechanical characteristics of the lignocellulosic fibers are controlled by the spatial adjustment of cellulose and the chemical treatments such as coupling agent addition, mercerization, or acetylation. The amorphous region of cellulose is more affected by chemical reagents compared with the crystalline region [70]. The mercerization for 72 hours to 96 hours was applied to coconut fibers with 5 wt% NaOH at 28°C by [71]. The mercerization improved elongation and tensile strength by 40% and 15%, respectively.

On the other hand, the high processing temperature of natural fiber reinforced polymer composites can negatively affect the corresponding mechanical properties,

color, and odor [64, 65]. Natural fiber degrades between 100°C and 300°C due to dehydration, oxidation, depolymerization, hydrolysis, discoloration, decarboxylation, and recrystallization [74]. The thermal stability and degradation degree of natural fibers depend on cellulose, hemicellulose, and lignin composition. Figure 12 represents the temperature ranges of typical natural fiber degradation [75]. Researchers recommend the use of natural fibers with low concentration of hemicellulose to avoid the degradation at lower temperatures [76]. Another recommendation for high thermal stability was associated with the use of natural fiber with high cellulose crystal size and crystallinity index [72]. Some fibers started to degrade immediately within short exposure of high processing temperatures. Flax fibers degrade above 170°C and show a drop in mechanical performance and polymerization [74].

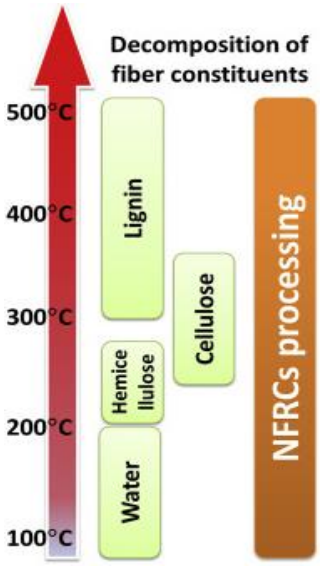

Figure 12: The decomposition temperature ranges of natural fibers constituents [77].

1.4.3 Date palm waste

The Middle East and North Africa regions are famous with the presence of date palm as a main agricultural product. The Arab world contains 84 million date palm trees out of 120 million date palm trees in the whole world. Date palm trees are concentrated in Egypt, Saudi Arabia, Iraq, Iran, Morocco, and the United Arab Emirates. A typical date palm tree produces 20 kilograms of waste in the form of dry leaves per year. The UAE produces 500,000 tons of date palm waste every year [3]. These are disposed of in landfills or burned in farms causing environmental pollution which can lead to global warming and its consequences due to the huge amounts of CO_2 produced from burning date palm waste.

Date palm wastes are excellent natural fillers to reinforce polymers because they are low in moisture content, high in volatile solids, and rich in polysaccharides cellulose reaching up to 40% by weight, and less than 10 weight percent of wax, pectin, fat and inorganic substances. Moreover, the world annual production of date palm trees is higher by 42% when compared with coir, and higher by 20% and 10% when compared with hemp and sisal, respectively. The polysaccharide cellulose is an inexhaustible polymeric raw material with attractive properties and structure. Cellulose can be extracted from different parts of date palm waste like fiber, rachis, and leaflet. Extracted cellulose from date palm waste can be used to reinforce different polymeric matrices like starch, Polylactic Acid, Polyvinyl Alcohol, and other polymers [4].

1.5 Polylactic Acid (PLA)

Polylactic Acid or Polylactide (PLA) is the maximum notably researched and utilized biodegradable and renewable aliphatic polyester. PLA has a demonstrated

potential both to substitute petrochemical-based polymers for packaging applications and as a main biomaterial for several applications in medicine [70, 71]. The constituent unit of PLA is Lactic Acid (2-Hydroxypropionic Acid, LA), found as two enantiomers, L-and D-Lactic Acid as shown in Figure 13. Lactic Acid can be produced by fermentation of sugars acquired from sustainable agriculture products like corn starch or sugarcane [80]. PLA has stereoisomers, for example, Poly D-Lactide (PDLA), Poly L-Lactide (PLLA), and Poly DL-Lactide (PDLLA) [78]. PLA is a non-toxic eco-friendly polymer and can be used in the human body because it is light and less hazardous. It is classified as safe for cutlery and food ware applications according to the United States Food and Drug Administration (FDA) [81].

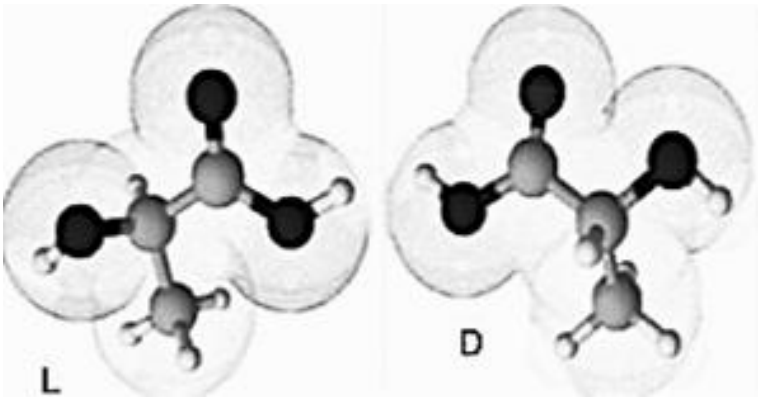

Figure 13: The chemical structure of L-and D-Lactic Acid enantiomers [82].

Low molecular PLA was synthesized by Carothers at DuPont Chemical Company in 1932 [81]. High molecular weight PLA was achieved by ring-opening polymerization. There are different approaches of PLA synthesis, none of them is straightforward or simple to execute, because its synthesis requires accurate control of polymerization period, weight, temperature, pH and the utilization of catalyst [82]. The polymerization of PLA as displayed in Figure 14 can take different processes such as, ring opening polymerization, direct methods of enzymatic polymerization and

azeotropic dehydration [83]. Direct and ring opening polymerization are the most utilized synthesis methods of PLA.

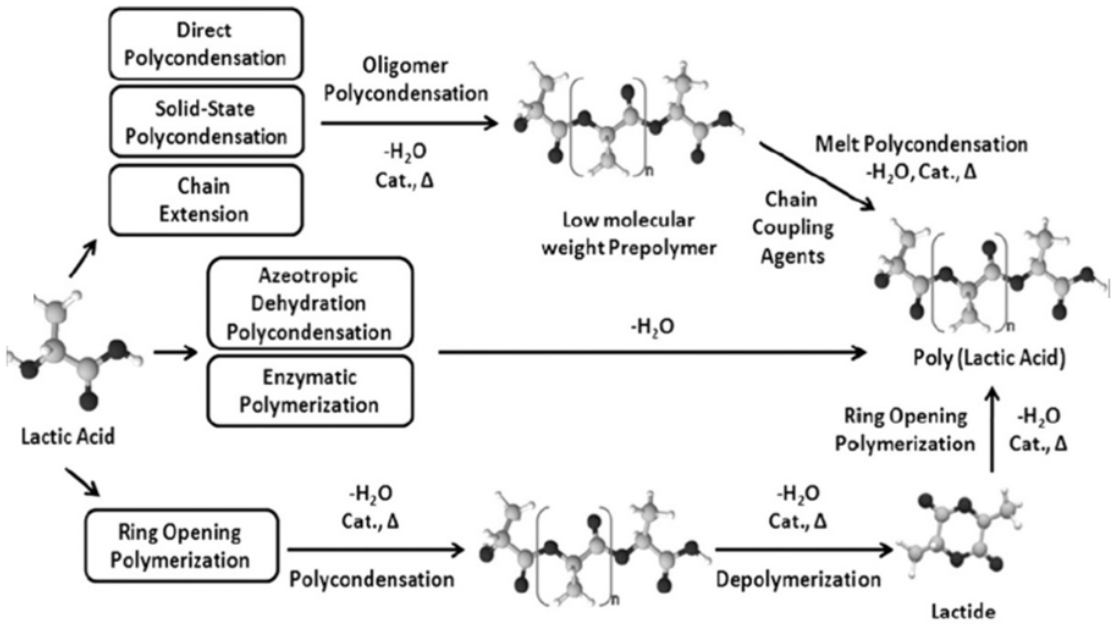

Figure 14: Synthesis techniques of PLA from Lactic Acid [82].

1.5.1 PLA compared to other biopolymers

The synthesis of PLA has various points of interest compared to other biopolymers [81]. PLA is mainly obtained from renewable resources such as corn, which makes it recyclable, biodegradable, and compostable [71, 76]. The synthesis of PLA requires the consumption of CO_2 [85]. PLA is highly recommended in biomedical applications because it is a biocompatible material in which it will not produce carcinogenic or toxic effects in nearby tissues. The thermal processability of PLA is better than other biopolymers like Poly Caprolactone (PCL), Polyhydroxyl Alkenoate (PHA) and Polyethylene Glycol (PEG). PLA can be processed by wide range of processes including injection molding, blow molding, thermoforming, film extrusion and fiber spinning [86].

The production of PLA requires 25–55% less energy compared to the production of petroleum-based polymers and predictions stated that the production energy of PLA will be reduced to 10% less energy in the future [27]. Semicrystalline PLA has higher mechanical properties than amorphous polymers by showing a tensile strength of 50–70 MPa, and flexural strength of 100 MPa [79, 80]. Table 2 shows that the tensile strength and elongation at break of PLA are similar to those of Polyethylene Terephthalate (PET). Despite the positive highlights, PLA has limitations too such as being brittle with less than 10% elongation at break [18], the slow degradation rate upon disposal in ambient outdoor conditions from 3 to 5 years [21] and relatively hydrophobic characteristics with no reactive side-chain groups for easy surface modifications and adhesion with other polymers. However, the thermal degradation, glass transition, and melting temperature of PLA are 200°C, 55°C and 175°C, respectively. The processing of PLA requires high temperatures of up to 190°C [88]. The degradation of PLA starts with the hydrolysis of backbone ester groups and its rate is affected by PLA crystallinity, molecular weight, and stereoisomeric content.

1.5.2 Plasticizers used to improve the ductility of PLA

Plasticizers are generally used to enhance processability, ductility, and flexibility of polymers. For semi-crystalline polymers such as PLA, a good plasticizer within 10 to 20 weight percent is needed to reduce the glass transition temperature, melting temperature and crystallinity [81, 82]. It is not preferred to use low molecular weight plasticizers due to their high mobility and migration within the PLA matrix. Another recommendation might be the use of non-toxic and biodegradable plasticizers for food ware applications. To enhance the ductility and elongation of PLA, it can be

blended with other less brittle polymers such as Polybutylene Succinate (PBS), Polycaprolactone (PCL) and Polybutylene Adipate-co-Terephthalate (PBAT) [91, 92].

PBAT is a completely biodegradable aliphatic-aromatic co-polyester with the ability to enhance the flexibility and reduce the brittleness of PLA. Because of the high cost of PLA and PBAT, other plasticizers, which are more efficient at relatively lower cost such as citrate esters have been suggested [93]. Citrate esters are nontoxic and can be used in medical, cutlery and food ware plastic applications. Also, the polar interactions among the ester groups of PLA and the citrate esters lead to good solubility of citrate esters within PLA matrix [94]. Triethyl Citrate (TEC) and Acetyl Tributyl Citrate (ATBC) are good candidates to successfully plasticize PLA, decrease glass transition temperature and improve the ductility. The effect of using TEC and ATBC with various compositions of up to 30 wt% on thermal, rheological and migration properties of PLA have been reported [95].

1.5.3 Natural fiber reinforced PLA composites

A group of researchers fabricated and studied a system of biodegradable composites from extrusion grade PLA (INGEO 2003D) and (3 wt% - 6 wt%) hemp fibers for use in automotive, construction, and packaging applications[96]. Whereas, a group of researchers developed a bio-composite from 20 wt% wood pulp fiber reinforced PLA [97]. PLA and wood fibers were processed by twin-screw extruder, then pelletized and used for injection molding. A multifunctional bio-additive called bioadimide was used to improve the composite heat distortion, fiber-matrix adhesion, flexural strength along with tensile modulus.

Moreover, Nuthong and co-authors examined the effect of the addition of three different abundant natural fibers up to 40% by weight to reinforce PLA to work as a

sustainable alternative to petroleum-based plastics in a variety of applications in Thailand [98]. The three natural fibers used in this investigation were bamboo fiber, coconut fiber and vetiver grass fiber. One weight percent of flexible epoxy was used as a surface treatment to the fiber prior to twin extruder processing and injection molding. Results revealed that the increase in the fiber content decreased the impact strength. The minimum reduction in impact strength was assigned to bamboo fiber-PLA when compared with the combinations of the two other types of fibers.

Chapter 2: Materials and Research Methods

2.1 Materials

The Polylactic Acid (PLA) used in this research was a general purpose Ingeo biopolymer (2003D) which was supplied by Nature Works LLC, Minnesota, USA as presented in Figure 15. This PLA is a high molecular weight of 181744 g/mol thermoplastic extrusion grade polymer that is made from renewable resources to be used in food packaging applications [35]. It is transparent with a specific gravity of 1.24, Melt Flow Index of 6 g/10 min at 210°C and tensile strength of 53 MPa based on the datasheet of Nature Works for Ingeo™ Biopolymer 2003D in 2018. The Triethyl Citrate (TEC) was supplied by Sigma-Aldrich and used as a plasticizer. Polybutylene Adipate-co-Terephthalate (PBAT) was supplied by Natur-Tec®, India and used as an alternative plasticizer to enhance PLA ductility, flexibility, and processability. Also, tap and saline water (37 ppt) were used in water uptake tests.

Figure 15: Pure PLA.

The date palm waste used in this study was obtained from Al Foah Farm in Al Ain which is managed by UAEU. The date palm waste (Figure 16) was collected as large pieces and classified as fiber, rachis, and leaflet. The rachis parts, which contained the highest amounts of cellulose compared with fiber and leaflets, were selected for this study. Rachis was washed to remove sand, dust, and other particles, followed by shredding to few-centimeter chips using a high-speed shredder (TEEBA, Date Seed Grinding Machine) as shown in Figure 17. The shredded rachis was further chopped using a lopper then dried in a laboratory oven at 80°C for 24 hours. The sample was then ground using (AJH, electric grain grinder SUS304) and sieved to 90- and 53-micron particle size using the corresponding sieve mesh with an electric shaker (MATEST, Auto Sieve Shaker).

Figure 16: Mixed date palm waste from the UAEU Al Foah Farm in Al Ain.

Figure 17: Date Palm Rachis preparations and size reduction. (a) rachis collection, (b) rachis shredding, (c) further chopping using a lopper, (d) size reduction by grinder, and (e) ground sample ready for sieving.

2.2 Cellulose extraction from date palm biomass

A weighed amount (10 grams) of the sieved biomass from rachis was placed in extraction thimble and inserted in the Soxhlet extraction apparatus as shown in Figure 18. About 150 ml of benzene and ethanol in a 2:1 ratio was used as the extraction solvent over a four to five hours period at the boiling point to remove any waxes, inorganic salts, proteins, and pectin using the method described by [91, 99]. At the end of the extraction, the solvent was evaporated from the extraction thimble. The dried sample after extraction was weighed and the amount of volatile compounds removed from the original biomass was determined.

The dried sample after extraction in the form of a solid mixture containing cellulose, hemicellulose, and lignin was transferred to a 250 ml beaker. Then 200 ml of 0.1 M HCl was gradually added. The beaker was placed on a heater at a temperature of 100°C for two hours with continuous magnetic stirring. After hydrolysis, the solution was filtered. At the end of the filtration step, the solution contained hemicellulose; keeping wet cellulose and lignin on the filter paper which was transferred to a petri dish for drying. In the last stage, the dried filtrate in the form of a solid mixture containing lignin and cellulose was transferred to a 250 ml beaker. Then 200 ml of 0.1 M NaOH was gradually added. The beaker was placed on a heater at a temperature of 100°C for two hours with continuous magnetic stirring. After NaOH treatment, the solution was filtered. At the end of the filtration step, the solution consisted of lignin; keeping wet cellulose on the filter paper which was transferred to a petri dish to dry and used later as a filler in the formation of the biodegradable composite.

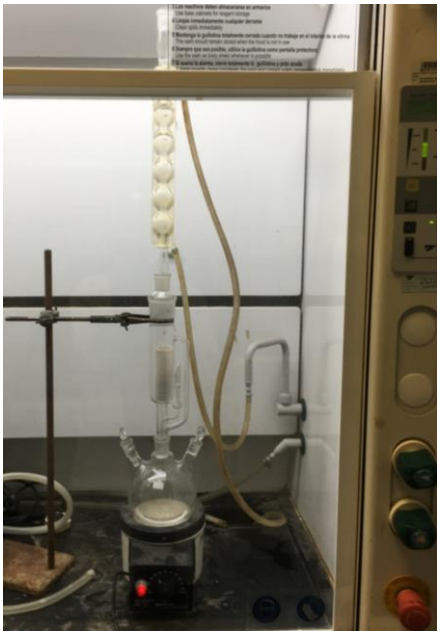

Figure 18: Soxhlet extraction apparatus.

2.3 Fabrication of composite samples

Sieved Date Palm Rachis (DPR) sample (53- and 90-microns) was added as a filler to the biodegradable polymer of Polylactic Acid (PLA) in three different compositions of 30%, 40% and 50% by weight. The DPR was not subjected to any chemical treatments or surface modifications to avoid the use of chemicals in food grade applications, reduce the production cost and save the energy used in cellulose extraction. Whereas 30 wt% of extracted cellulose were used to reinforce PLA. Melt mixing was performed using a two-screw extruder (MiniLab HAAKE Rheomex CTW5, Germany) at a screw speed of 140 rpm (Figure 19a). The control sample was prepared by blending pure PLA under the same conditions. Different parameters were varied including melting temperature, plasticizer type and mixing duration. It was observed that if biomass stays in a closed system for a long time, it undergoes partial pyrolysis. Different extruder mixing trials for 30% DPR-PLA composite shows that the best composite color with a recovery of 79.9 wt% and output thickness of 0.15 cm was produced by the melting of PLA at 180°C for 7 minutes followed by the addition of DPR to be mixed with PLA for 3 minutes.

Figure 19: 30% DPR-PLA composites fabrication using two screw extruders with different mixing times. (a) 7 min PLA, 3 min biomass, (b) 5 min PLA, 5 min biomass, and (c) 3 min PLA, 7 min biomass.

The produced composite was distributed in a cutlery mold and hot pressed for 15 minutes using a Carver's press machine (Carver Lab Presses, mode l4386) under 5000 psi pressure at the same temperature (180°C) used in the melt mixing extruder to prepare biodegradable cutlery such as a knife. However, the extruded bio-composite was re-melted via (HAAKE MiniJet Pro, Injection Molding Machine) in which the homogenous molten plastic was injected at high-pressure of 500 bars to fill the 80°C closed mold cavity of certain shape in 15 seconds to produce lab test specimens such as dumbbell-shaped specimens (Figure 20) for use in tensile testing. The prepared DPR-PLA composites were subjected to different thermal, mechanical, and physical tests based on ASTM or ISO.

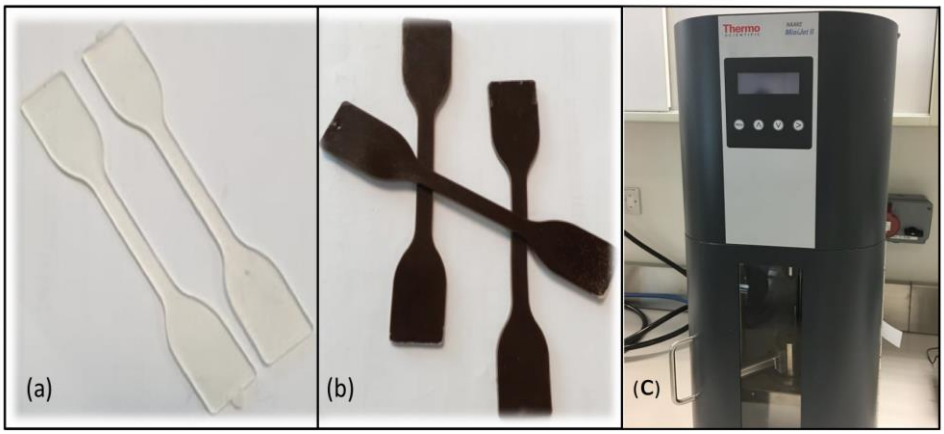

Figure 20: Dumbbell-shaped test specimens of (a) PLA and (b) 30% DPR-PLA composite prepared by (c) injection molding.

2.4 Physical and morphological characterization

2.4.1 Scanning Electron Microscopy (SEM)

Scanning Electron Microscopy (JEOL-JCM 5000 NeoScope) was used to observe the surface morphology of the DPR biomass, PLA, and prepared biodegradable composite samples. Using double sided carbon tape, the composite was placed on an aluminum pin mount adapter. The sample was sputter coated with gold using a sputter coater to avoid electrostatic charging during examination. The SEM images of the filler particles in the polymer matrix were recorded at different magnifications and developed at a high vacuum mode with an acceleration voltage of 5 kV.

2.4.2 Fourier Transform Infrared Spectrometry (FTIR)

Fourier Transform Infrared Spectrometry (ASTM E168, E1252) was used for identifying samples by their ability to absorb infrared light at different frequencies to produce a unique "spectral fingerprint". The DPR biomass, PLA and PLA-based

composites were scanned in the frequency range of 500 to 4000 cm^{-1} at a resolution of 4 cm^{-1} [100].

2.4.3 Water uptake test

Water absorption tests are carried out for PLA and DPR-PLA optimum composite samples in saline water with 37 ppt [101], tap water at room temperature and hot water according to ASTM D-570-98. Three specimens for each water type were tested. Tensile specimen was used with a thickness of 2 mm, a length of 73.5 mm with variable width to mimic the cutlery shape and to be able to fairly compare the biodegradation in tap and sea water with that in soil after 4 months. In the Long-Term Immersion tests in tap and seawater at room temperature, the specimens were removed from the water beakers at the end of the 24 hour, wiped off with a dry cloth, weighed to the nearest 0.001 g immediately using an accurate digital balance and then returned back in the water. The weighing was repeated after the first week, then every two weeks. While in the immersion at 50°C, the water beakers were kept in a hot water bath to maintain the water temperature at 50°C for 48 hours as presented in Figure 21. The water retention percentages (weight gains) were calculated as a function of initial weight (W_0) using the following expression:

$$W(\%) = \frac{W_t - W_0}{W_0} \times 100$$

Figure 21: Water uptake of DPR-PLA composite during the immersion (a) at room temperature tap water and (b) at 50°C in hot water bath for 48 hours.

2.4.4 Biodegradability test

Biodegradation of the optimum DPR-PLA composites under real soil conditions was carried out at the experimental soil located in the UAEU garden. The percentage of weight loss of PLA based composites and commercial samples during the burial in soil were recorded after 4 months. Figure 22 shows the burial of composite samples in a depth of 5 cm and 22 cm of dry and watered soil. The wet soil was periodically watered to imitate the real natural soil while the other soil was kept dry as environmental control media.

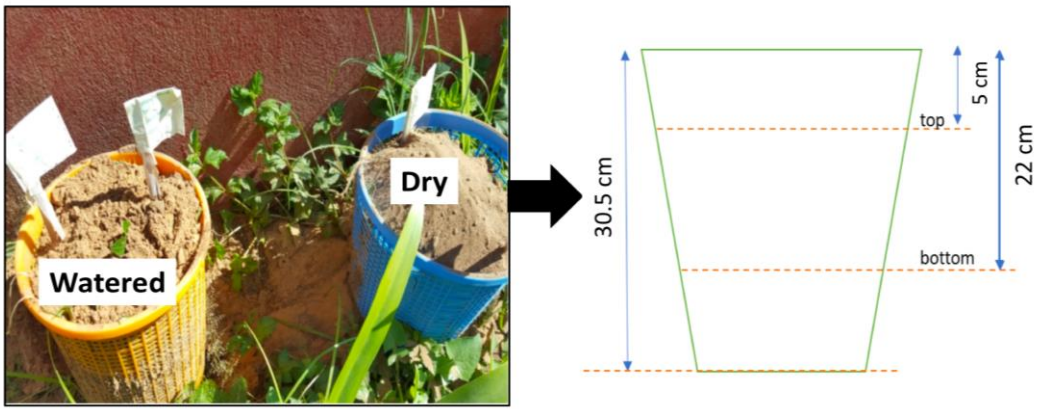

Figure 22: Burial of DPR-PLA composites in 5 cm and 22 cm depth of dry and watered soil.

2.5 Thermal characterization

2.5.1 Thermogravimetric Analysis (TGA)

Thermogravimetric analysis was used to determine the degradation temperature of the DPR biomass, PLA and PLA-based composites in a thermogravimetric analyzer (Q-50, TA Instruments, USA). Under nitrogen atmosphere supplied as 100 mL/min, the samples of 10-15 mg were heated from 20℃ to 800°C at a heating rate of 10°C/min.

2.5.2 Differential Scanning Calorimeter (DSC)

DSC (Discovery DSC 25, TA Instruments, USA) was used to determine the melting temperature of about 5 to 7 mg sample of PLA and PLA-based composites. The samples were heated up to 200°C in an inert nitrogen atmosphere. However, the melting temperatures (T_m), glass transition (T_g), and cold crystallization temperature (T_{cc}) were recorded from the second heating from 25°C to 200°C at 10°C/min.

2.6 Mechanical characterization

2.6.1 Melt Flow Index (MFI)

The change in Melt Flow Index (MFI) of PLA with the addition of Date Palm Rachis biomass waste was measured using XRL-400 series Melt Flow Index. MFI is simply the mass flow rate expressed in grams per 10 min under a constant load of 2.16 kg according to ISO 1133 at the melting point of 180℃. A weight of 5 g from the extruder output was broken into small pieces to be inserted in the barrel of the MFI machine. The re-melted bio-composite was ejected discontinuously in an approximately equal amount from the MFI die using an automatic cutter when the

cycle time of 10 seconds was completed. Finally, the melted samples shown in Figure 23 were measured using a digital balance and the average was calculated in grams per 10 seconds. Then MFI of PLA and DPR-PLA composites was then calculated in grams per 10 minutes.

Figure 23: Extruded DPR-PLA composite was broken into small pieces to be inserted in the barrel of the MFI machine.

2.6.2 Tensile strength test

Shimadzu Universal Testing Machine was used to determine the tensile properties of the PLA and the optimum biodegradable composite after plasticization as shown in Figure 24. In order to perform this test, dumbbell-shaped test specimens were prepared by re-melting the extruded bio-composites using HAAKE MiniJet Pro, Injection Molding Machine.

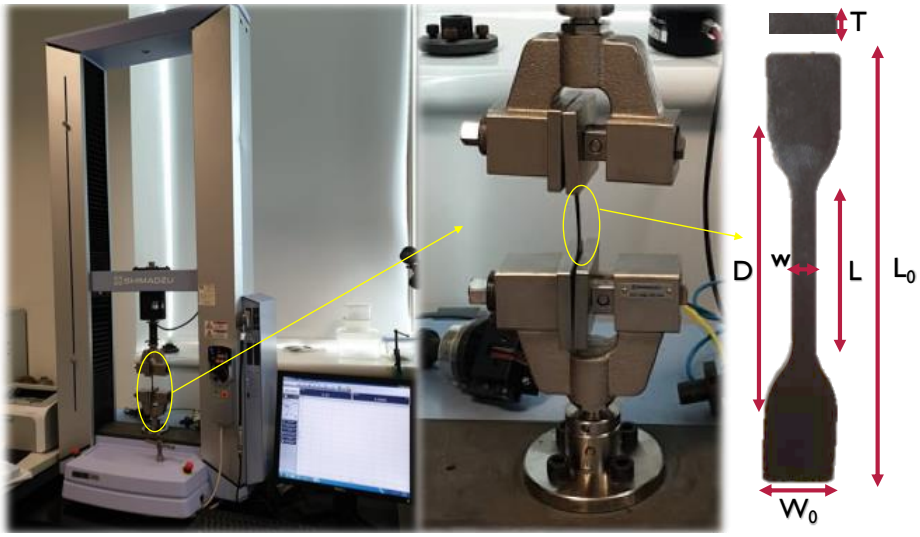

Figure 24: Tensile properties determination of the PLA and the Plasticized PLA-based composites using dumbbell-shaped specimens. The sample dimensions are: T=2 mm, w_0=12 mm, w=4 mm, L=30 mm, D=45 mm and L_0=73.5 mm.

Chapter 3: Results and Discussions

3.1 DPR-PLA composites

3.1.1 Thermogravimetric Analysis (TGA)

In order to avoid possible thermal degradation, the thermal characterization of any pure materials and their composites is a critical step before polymer processing. Figure 25 shows the derivative weight changes versus temperature curves of PLA, DPR and their fabricated three bio-composites (with a biomass content of 30 wt%, 40 wt% and 50 wt%) and their corresponding weight losses. The first weight loss for DPR and the three bio-composites is between 60°C and 100°C which corresponds to water vaporization from the wall structure, void space and the interfacial bonding between biomass and PLA matrix [102].

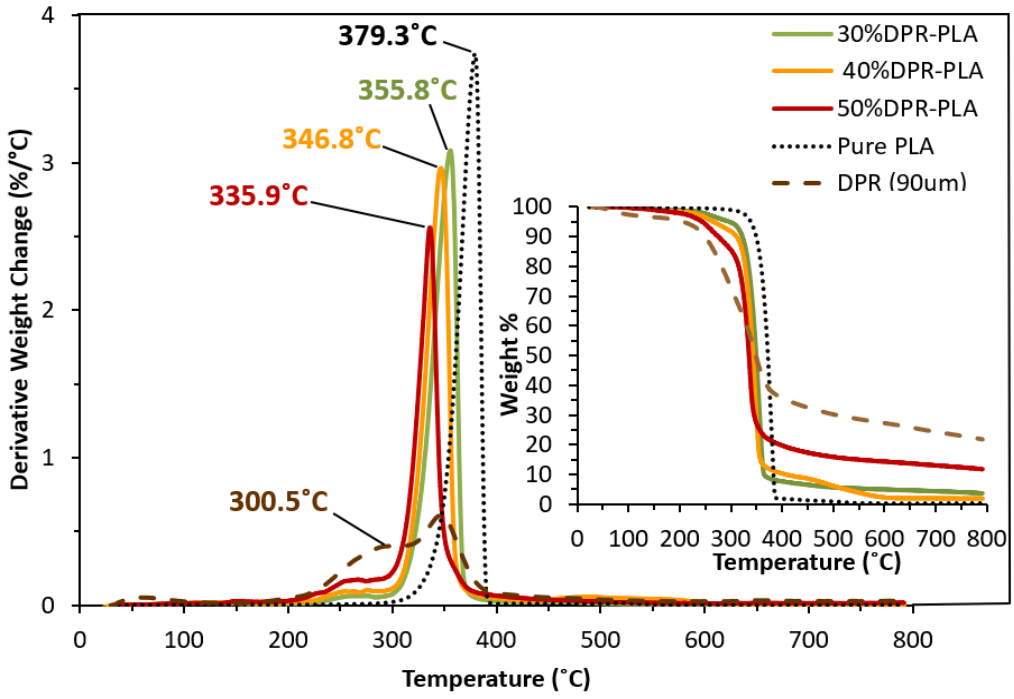

Figure 25: Derivative weight change and TGA plots of Pure PLA and DPR-PLA composites.

The DPR exhibits two phases of degradation as presented in Figure 25. The first phase has a weight loss of 27.4% at approximately 300.5°C. This phase is classified by the decomposition of pectin, cellulose, and hemicellulose at the same time [103]. The second phase has additional weight loss of 25.8% at around 353.9°C which can be explained by the decomposition of lignin. The derivative weight change and TGA plots of PLA, cellulose and 30% cellulose-PLA composite are presented in Figure 26. The extracted cellulose shows one phase of degradation at 306.1°C, thus confirming the agreement with the previous TGA findings regarding phase one of the DPR degradation. The DPR biomass indicates a good thermal stability by showing the highest final remaining residue of about 23 wt% at 800°C. On the other hand, the extracted cellulose shows less thermal stability compared with full Date Palm Rachis biomass by exhibiting a final remaining residue of about 4.8 wt%.

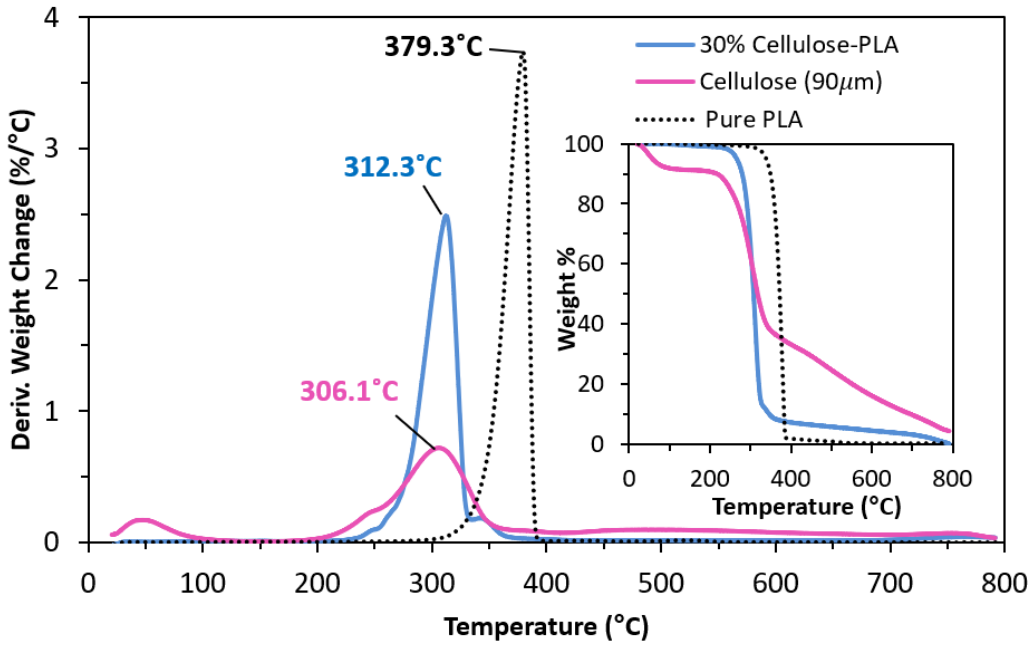

Figure 26: Derivative weight change and TGA plots of PLA, cellulose and 30% cellulose-PLA composite.

Figure 25 shows that the weight loss of 5% of PLA occurs at about 338.9°C while the DPR exhibits a 5% weight loss at about 206.3°C. Figure 26 shows that the extracted cellulose has a 5% weight loss at 57.0°C which is not preferable in extruder processing. This is due to the fast-partial pyrolysis and the undesired color change. Based on these results, the processing temperature was held below 200°C to prevent the thermal degradation of DPR in the PLA matrix. Figure 25 clearly proves that the pure PLA has no weight loss at 100°C, indicating the relative absence of water molecules. PLA presents 75.4% weight loss at 379.285°C and a final remaining residue of 0.3 wt% as shown in Figure 25, which is in agreement with the results obtained by [104]. In addition, the thermal degradation process of pure PLA can be explained by two steps, beginning with dehydration followed by chain scission [105]. Moreover, the three bio-composites demonstrated an intermediate level of thermal stability that is noticeably lower than that of pure PLA and higher than the thermal stability of DPR.

The increase of the biomass content in the PLA-composite matrix shifts the degradation temperatures of the bio-composites to lower regions towards the biomass degradation temperature. The bio-composites of PLA with a biomass content of (30 wt%, 40 wt% and 50 wt%) have degradation temperatures of 355.762°C, 346.750°C and 335.998°C, respectively whereas their corresponding weight losses are 83.6%, 71.1% and 52.4%, respectively as shown in Figure 25. In addition, Figure 25 shows that the derivative weight loss of the pure PLA was significantly higher than all DPR-PLA composites, while DPR revealed a minimum derivative weight loss. The observed derivative weight loss trend agreed with other researchers [106]. The 30% cellulose-PLA composite shows relatively lower degradation temperature of 312.3°C

with a lower weight loss of 60.9% as presented in Figure 26 when compared to 30% DPR-PLA composite.

3.1.2 Differential Scanning Calorimetry (DSC)

The DSC curves of PLA and PLA based composites with DPR content of 30 wt%, 40 wt% and 50 wt% are presented in Figure 27 and their corresponding phase-transition data are recorded in Table 4. The heating range was chosen to be from 20°C to 200°C according to the TGA results that suggested the fabrication of the bio-composites below 200°C to avoid thermal degradation. However, the second heating curves were recorded due to the existence of obvious thermal peaks, while the first heating scan played an essential role in removing the thermal history of the polymer. When polymers are cooled below their glass transition temperature, they are observed to be hard and brittle like glass as clarified in Figure 28. Figure 27 shows that the glass transition temperature of the amorphous phase of pure Polylactic Acid (PLA2003D) is 59.1°C which agrees with other researchers as they obtained it as 59.5°C upon the second heating [107]. The cold crystallization peak at 122.05°C and the melting peak at 149.93°C were also in agreement with the reported values in the literature [104].

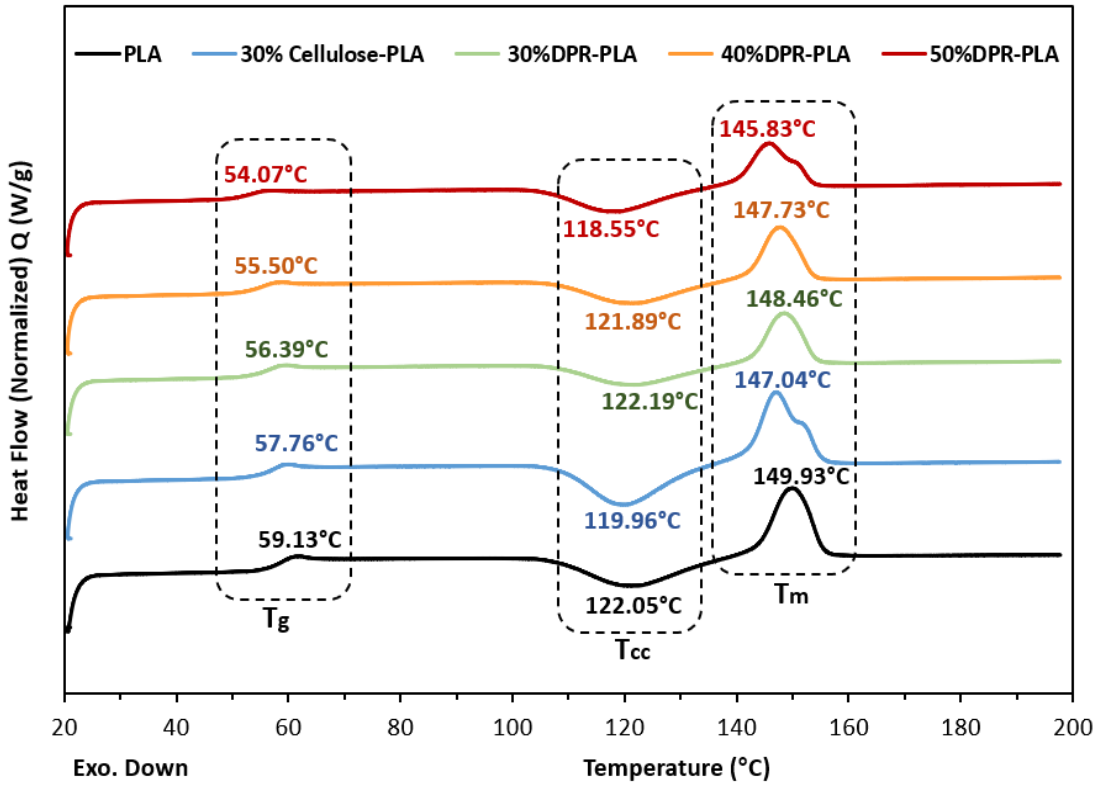

Figure 27: The DSC thermograms of PLA and PLA based composites with a DPR content of 30 wt%, 40 wt% and 50 wt% and with cellulose content of 30 wt% upon the second heating at 10°C min^{-1}.

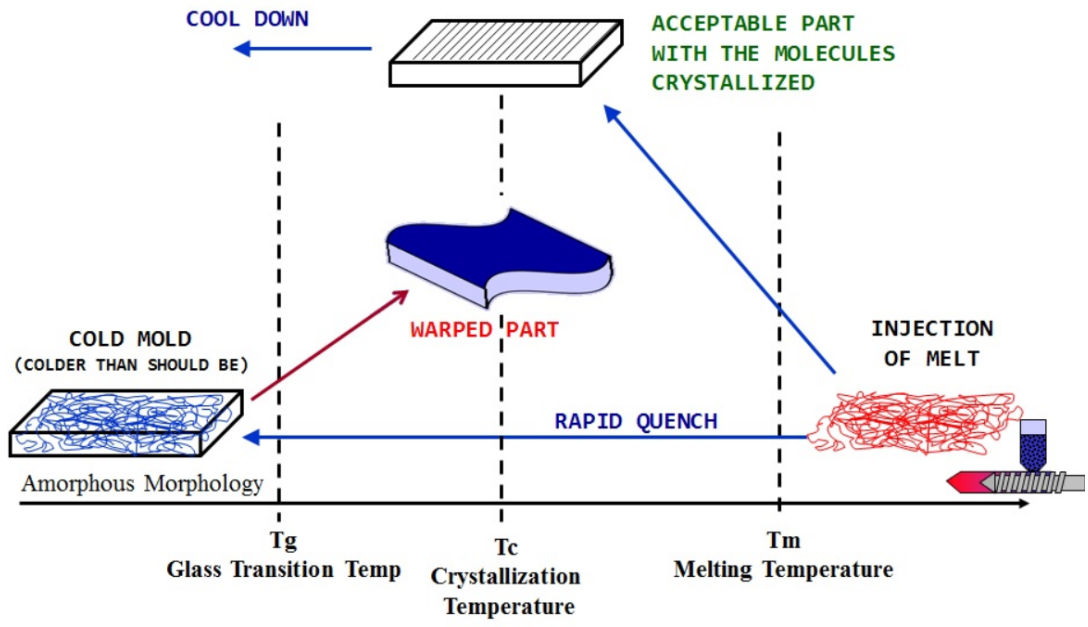

Figure 28: The thermal behavior of a molten polymer during various cooling paths [108].

The glass transition temperatures of the PLA based composites with a biomass content of 30 wt%, 40 wt% and 50 wt% shifted to slightly lower temperatures of 56.39°C, 55.50°C and 54.07°C, respectively as shown in Figure 27. Also, the cold crystallization temperatures of the bio-composites reduced insignificantly compared to pure PLA. This reduction indicates the nucleation activity of the biomass as a filler [109]. Moreover, the decrease in T_{cc} is followed by a slight drop in the melting temperature (T_m) of the PLA with the addition of 50 wt% biomass from 149.93°C to 145.83°C. The slight decrease in T_g, T_{cc} and T_m of the PLA upon the increase in biomass content is explained by the resultant weaker interactions. This can lead to the increase in mobility that promotes the increase in the degree of crystallinity [110]. Furthermore, Table 4 clearly displays that the range of melting enthalpy was equal to the cold crystallization enthalpy. This indicates that the DPR-PLA matrix was amorphous before heating in the DSC [111]. The 30% cellulose-PLA composite showed a quite similar T_g, T_{cc} and T_m but relatively higher ΔH_{cc}, and ΔH_m when compared to 30% DPR-PLA composite as displayed in Figure 27 and Table 4.

Table 4: The calorimetric data for PLA and PLA based composites with a DPR content of 30 wt%, 40 wt% and 50 wt% and with cellulose content of 30 wt% upon the second heating at 10°C min^{-1}.

Sample	T_g (°C)	T_{cc} (°C)	T_m (°C)	ΔH_{cc} (J/g)	ΔH_m (J/g)
Pure PLA	59.13	122.05	149.93	21.21	22.86
30% Cellulose - PLA	57.76	119.96	147.04	23.591	23.87
30% DPR - PLA	56.39	122.19	148.46	14.30	14.99
40% DPR - PLA	55.50	121.89	147.73	14.18	17.06
50% DPR - PLA	54.07	118.55	145.83	14.10	14.74

3.1.3 Fourier Transforms Infrared Spectroscopy (FTIR)

FTIR analysis was performed on pure PLA and the composite samples after the addition of Date Palm Rachis biomass to PLA. The infrared spectrum obtained for the DPR is shown in Figure 29. The DPR exhibits typical vibration bands of various chemical functional groups that are found in cellulose, hemicellulose, and lignin. The vibration of the OH bond in the biomass spectrum is directly related to the broad and strong absorption band between 3200 and 3500 cm^{-1} as shown in Figure 29. The peak at 2916.324 cm^{-1} is assigned to the vibration of the asymmetrical stretching of the CH bond in the biomass [112]. The absorption band at around 1735.138 cm^{-1} can be attributed to the carbonyl group (CO) and the ester group with stretching vibration in hemicellulose [113]. In addition, the lignin bands at 1247.236 cm^{-1} to 1400 cm^{-1} are indicative of OCH_3 and CC bonds respectively [67]. At 1423.691 cm^{-1}, the absorbance is due to the existence of CH deformation in lignin, and the symmetrical bending of CH_2 in cellulose [114]. However, the bending vibration of the CH group on the aromatic ring at 1371.14 cm^{-1} is assigned to the hemicellulose and cellulose [113] .

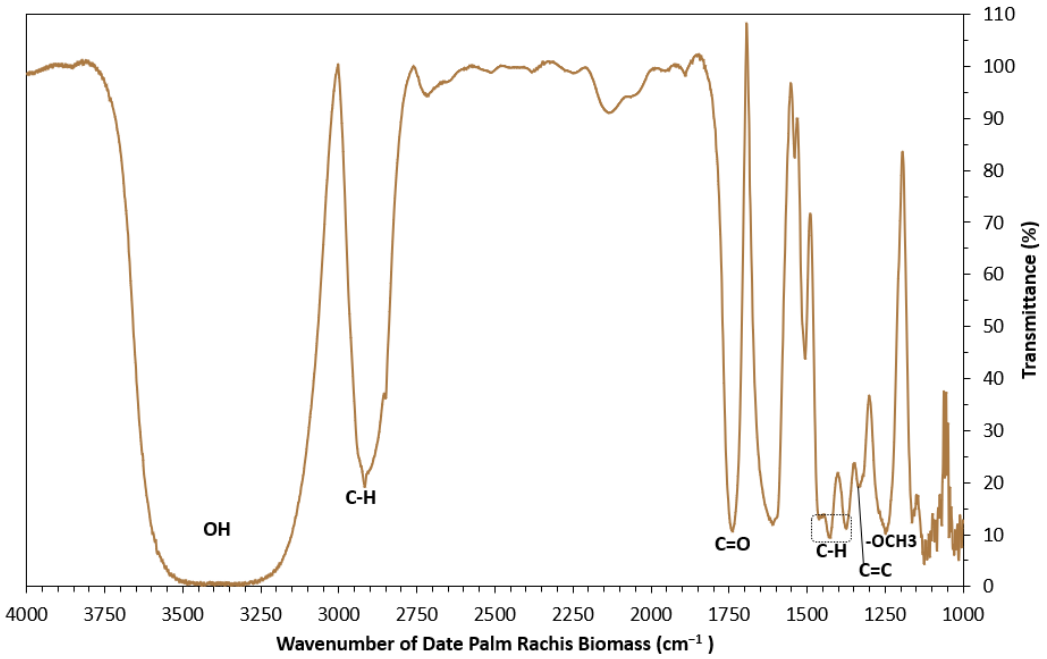

Figure 29: FTIR spectra of DPR.

To investigate the presence of potential interfacial interaction between PLA and DPR biomass, FTIR experiments were conducted and compared with those of pure PLA as shown in Figure 30. The O–H peak in PLA is observed at 3295.268 cm^{-1}. The bands observed at 2916.32 cm^{-1} and 2848.35 cm^{-1} can be linked to the stretching of symmetric and asymmetric C—H in CH_3. However, three main FTIR spectra regions can be observed for PLA and PLA-based composites. The first region at 1744.298 cm^{-1} is linked to carbonyl (-C=O) stretching peak in PLA. The second region is assigned to the -CH-O- group (–C-O- stretching bond) in PLA at 1180.704 cm^{-1}. The last region consists of three distinctive peaks, which are attributed to the stretching vibrations in -O-C=O group (-C-O-) at 1128.153, 1081.870 and 1039.444 cm^{-1}. The bands at 866.846 cm^{-1} and 752.584 cm^{-1} are related to the PLA amorphous and crystalline phases. These FTIR results are consistent with the findings of Popa and co-authors [115]. The O–H peak in PLA at 3295.268 cm^{-1} became broader and shifted towards

marginally lower wavenumbers in the three DPR-PLA composites as shown in Figure 30. This change may be attributed to the "free" groups of hydroxyls, which bind with hydrogens [105, 106].

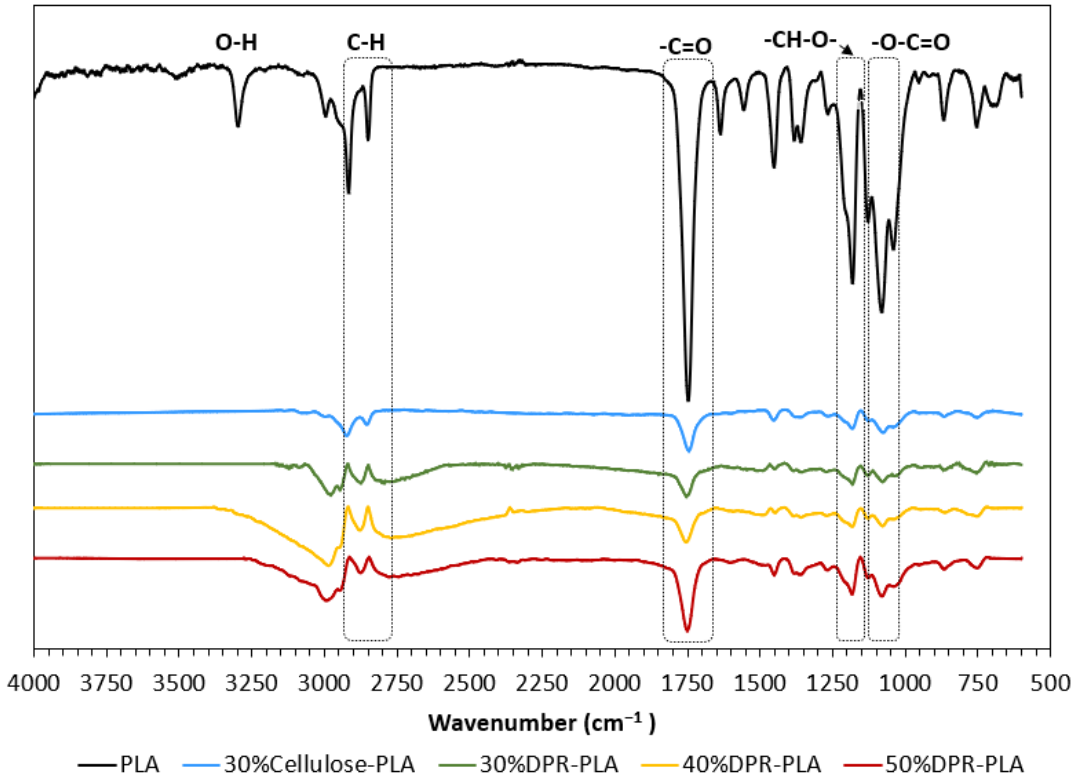

Figure 30: FTIR spectra of PLA and PLA based composites.

The most important changes in the bio-composites compared with pure PLA are found in the carbonyl (C=O) stretching vibration at 1744.298 cm^{-1}. This peak slightly shifted towards low wavenumbers by the increase in the biomass content of the DPR-PLA composite. Cellulose possess a higher number of -OH groups compared with other biomass components such as hemicellulose, pectin and waxy substances. Due to this characteristic, the C=O bond in the PLA can develop cellulose hydrogen bonds by its carboxyl and terminal hydroxyl groups [118]. This interaction causes a sudden decrease in intensity of the C=O peak in 30% DPR-PLA composite [119, 117].

However, the increase in the biomass content from 30 wt% to 50 wt% causes the gradual rise in the intensity of C=O stretching peak as shown in Figure 30. This is because of the esterification reaction between –OH of the biomass, the carbonyl (C=O) and the terminal –COOH group in the PLA [120].

3.1.4 Scanning Electron Microscopy (SEM)

The morphology and phase adhesion in the PLA matrix, DPR, and fractured surfaces of their bio-composites produced by injection molding were studied. Figure 31 (a) shows SEM micrographs of PLA resin, presenting brittle nature with continuous phase and smooth exterior with several stream-like waxy cracks. Analogous SEM images were observed for PLA and cellulosic fibers by [121]. The rachis biomass was grinded to 53 μm (Figure 31 (b)) and 90 μm (Figure 31 (c)). It can be seen that biomass appears as aggregates of entities with some nanofibrils on the surfaces of the biomass particles. These observations could be an indication that the biomass particles are agglomerations of thousands of individual biomass nanofibrils.

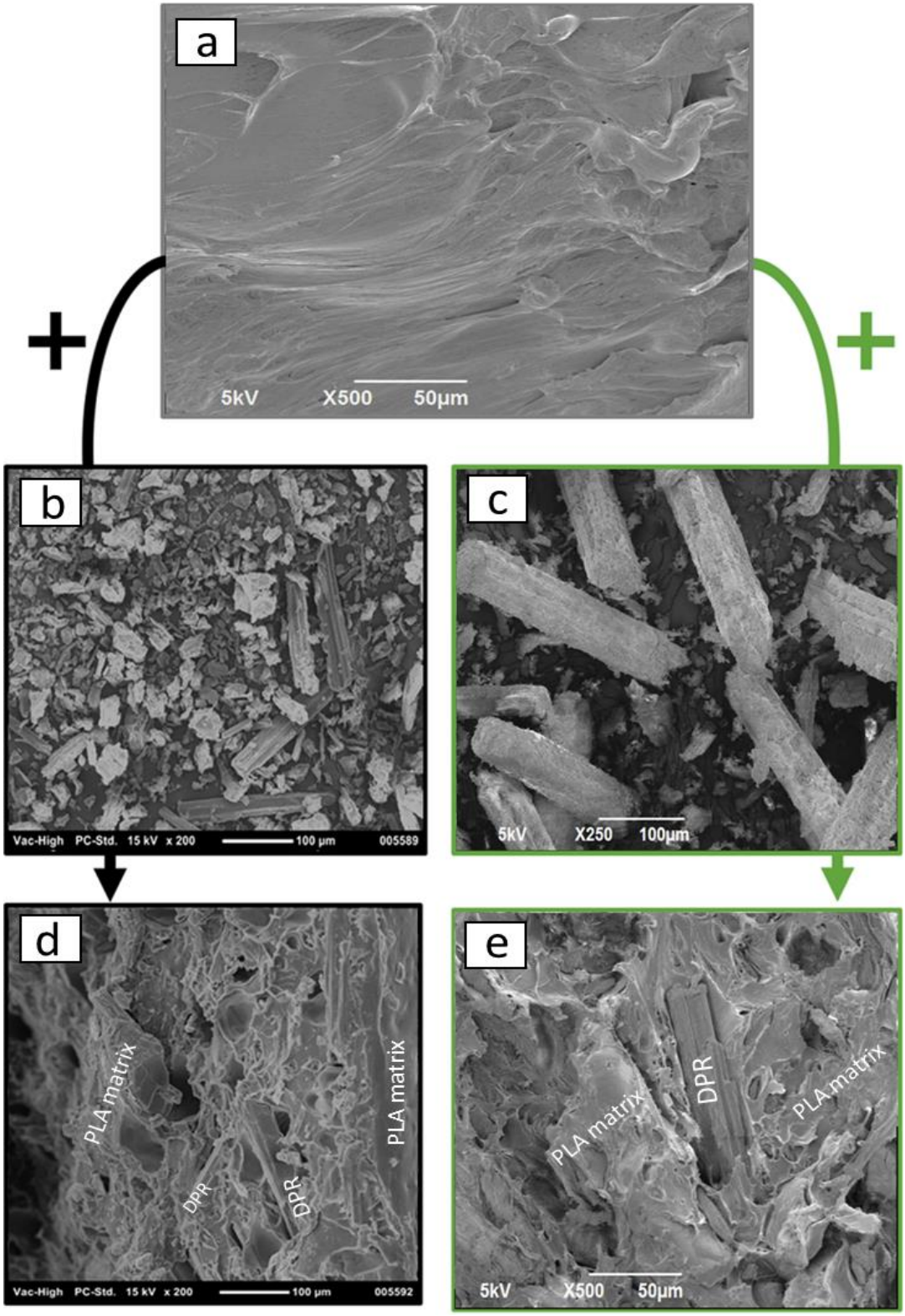

Figure 31: SEM images of (a) pure PLA, (b) DPR (53 µm), (c) DPR (90 µm), (d) 30% DPR (53 µm)-PLA, and (e) 30% DPR (90 µm)-PLA composite.

SEM was used to explore the surface morphology and distribution of the biomass filler in the PLA matrix. A uniform dispersion of the 30 wt% DPR filler with the particle size of 53 μm (Figure 31 (d)) and 90 μm (Figure 31 (e)) in the PLA matrix was observed. Another finding was that the biomass still existed as thin fibril bundle aggregates with a good fiber orientation, and no real bundle separation occurred during the extrusion stage. Since both particle sizes of the biomass gave similar morphology and adhesion in the PLA matrix, the 90 μm biomass was used in the fabrication of PLA based composites as larger size particles require less energy for particle size reduction. On the other hand, the SEM image in Figure 32(b) revealed relatively better adhesion of the extracted cellulose (90 μm) to the PLA matrix compared to the untreated DPR shown in Figure 31(e). The extracted cellulose seems to be uniformly distributed in the PLA matrix.

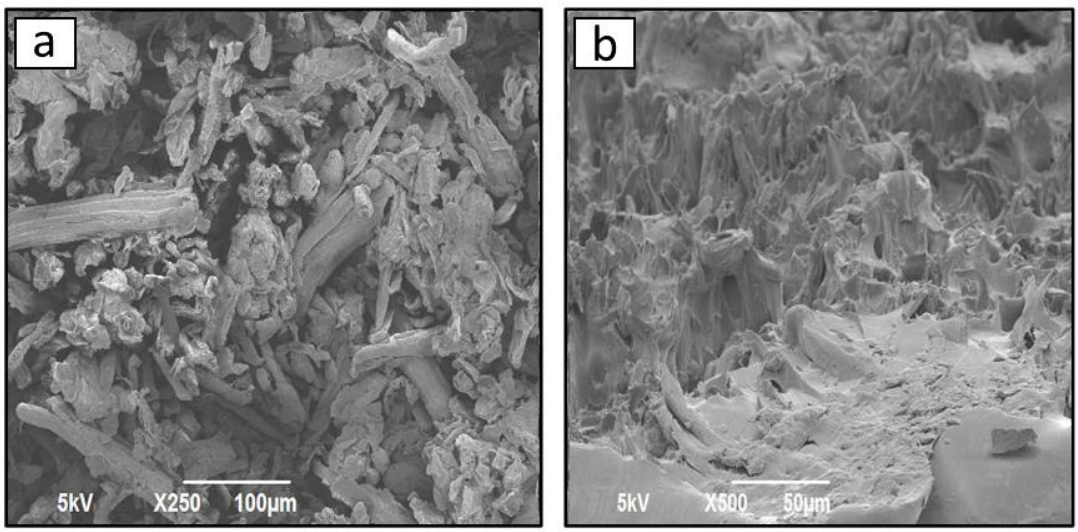

Figure 32: SEM images of (a) cellulose (90 μm) and (b) 30% cellulose (90 μm)-PLA composite.

The SEM micrographs of 40 wt% and 50 wt% DPR-PLA composites are presented in Figure 33. Both bio-composites show that the fibril bundles surface in the biomass are covered by the PLA. However, the extent of coverage for 40 wt% and 50 wt% composite is lower than that of 30% DPR-PLA composite. The addition of 40 wt% and 50 wt% biomass to the PLA develops a slightly rougher and coarser surface. This may lead to a noticeable increase in brittleness and the absence of ductility nature, which could be worse for the 50% DPR-PLA composite due to the extra accumulation of the biomass in certain points and voids within the bio-composite and the insufficient quantity of PLA to offer real wettability when biomass is increased to 50 wt%. Furthermore, the observed voids on the SEM images may be due to the existence of water that might be formed during the fabrication process [122].

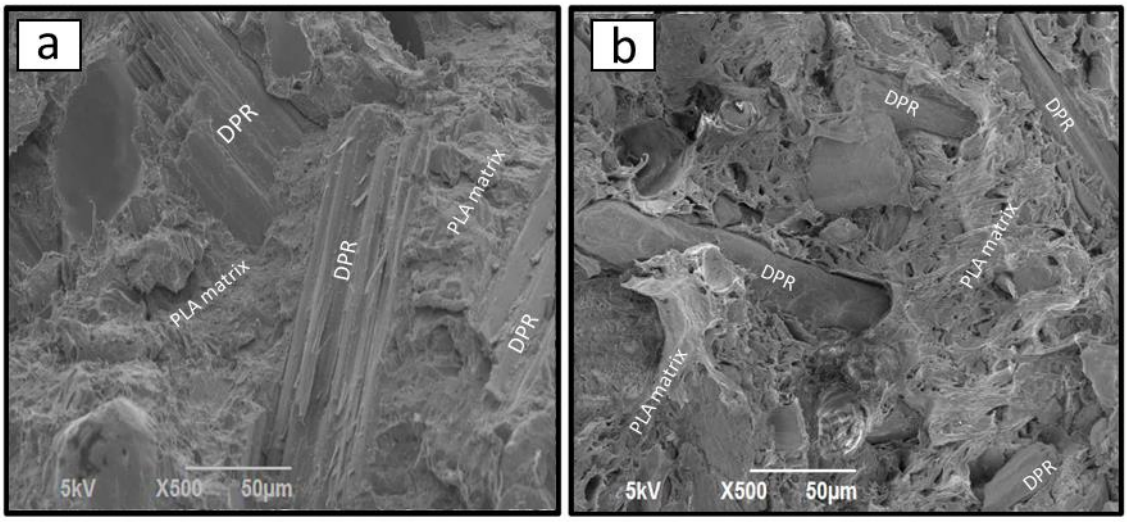

Figure 33: SEM images of (a) 40% DPR 90 µm-PLA composite and (b) 50% DPR 90 µm-PLA composite.

3.1.5 Melt Flow Index (MFI)

The changes in Melt Flow Index (MFI) with the addition of Date Palm Rachis is illustrated in Figure 34. The MFI of PLA was obtained to be 7.09 g per 10 min, which agrees with the reported values by Nature Works LLC and other researchers [123] . The addition of the biomass (30 wt%, 40 wt% and 50 wt%) to PLA causes a gradual increase of the MFI to 16, 31.57, and 54.78 g/10 min, respectively. This indicates the growth of extrusion throughput because a greater mass of the bio-composite flows through the extruder die at a particular time. A significant increase in the MFI from 14.15 to 68.60 g/10 min was observed in the PLA matrix with the addition of 30 wt% of ground chestnut shell [124]. On the other hand, the 30% cellulose-PLA composite showed an undesirable MFI of 79.15 g/10 min, which is five times that of the 30% DPR-PLA composite as presented in Figure 34.

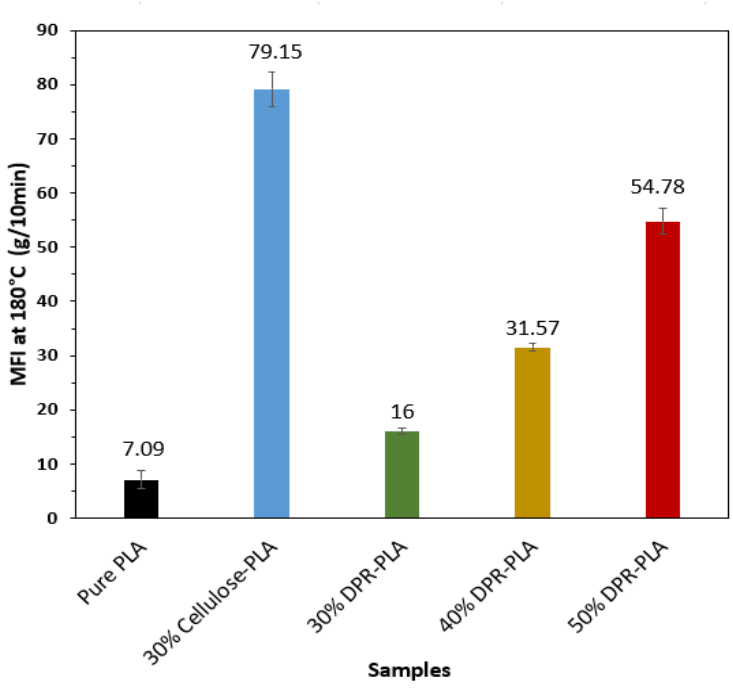

Figure 34: Melt flow index of PLA and PLA based composites at 180°C (g/10 min).

When the amount of biomass is increased in the PLA based composite, small particles of the biomass can penetrate and accumulate in the PLA matrix as displayed in the SEM images in Figure 33, thus developing easer slip and flow of the PLA matrix. The results of the Melt Flow Index are well correlated with the previous DSC findings as well. DSC results showed a slight decrease in T_g, T_{cc} and T_m of the PLA by the increase of the biomass content because of the resultant weaker interaction that leads to the increase in the mobility. The 30% DPR-PLA composite showed lower MFI when compared to the other two PLA based composites with 40 wt% and 50 wt% of DPR. For easier cutlery fabrication and processing in large scale extruders and injection molding machines, 30% DPR-PLA composite was selected and tested in one of the plastic production industries in China as shown in Figure 35.

Figure 35: Industrial fabrication of cutlery from 30 wt% DPR-PLA composite. (a) mixed PLA and DPR, (b) melt mixing extrusion, (c) two plates with mold cavity of spoons shape ready for injection molding, and (d) spoons collection after the two plates separation of the mold.

3.2 DPR-PLA composites with plasticizers

3.2.1 Thermogravimetric Analysis (TGA)

Thermogravimetric analysis was carried out on the plasticized 30% DPR-PLA composites to investigate the effect of the addition of Triethyl Citrate (TEC) and Polybutylene Adipate-co-Terephthalate (PBAT). Three levels of these plasticizers (1 wt%, 5 wt% and 10 wt%) were used and the results are shown in Table 5 and Figure 36. TGA analysis revealed that the maximum decomposition temperatures of all the plasticized composites are lower than both neat PLA and unplasticized 30% DPR-PLA composite. The degradation temperatures of the plasticized composites at maximum weight loss were shifted from 355.8°C (30% DPR-PLA) to 336.7°C and 332.9°C with the addition of 10 wt% TEC and 10 wt% PBAT, respectively. A similar trend was observed by Mounira Maiza and co-workers after plasticizing PLA with TEC up to 30 wt% [95]. All plasticized composites with TEC and PBAT show good thermal stability and their thermal degradation temperatures are higher than the controlled processing temperature of 180°C.

Table 5: Thermogravimetric analysis of the plasticized 30% DPR-PLA composites with three levels of TEC and PBAT.

	$T_{5\%}$ (°C)	T_{max} (°C)	$T_{50\%}$ (°C)	Stability (%)
PLA	338.9	379.3	370.4	98.1
30% DPR+PLA	291.9	355.8	347.8	93.8
30% DPR+PLA+1% TEC	256.7	342.0	332.7	92.3
30% DPR+PLA+5% TEC	207.6	333.0	324.6	85.7
30% DPR+PLA+10% TEC	205.1	336.7	326.8	85.4
PBAT	364.9	403.9	400.0	99.0
30% DPR+PLA+1% PBAT	243.3	330.3	324.4	92.1
30% DPR+PLA+5% PBAT	246.9	330.3	324.4	92.1
30% DPR+PLA+10% PBAT	252.8	332.9	328.4	92.6

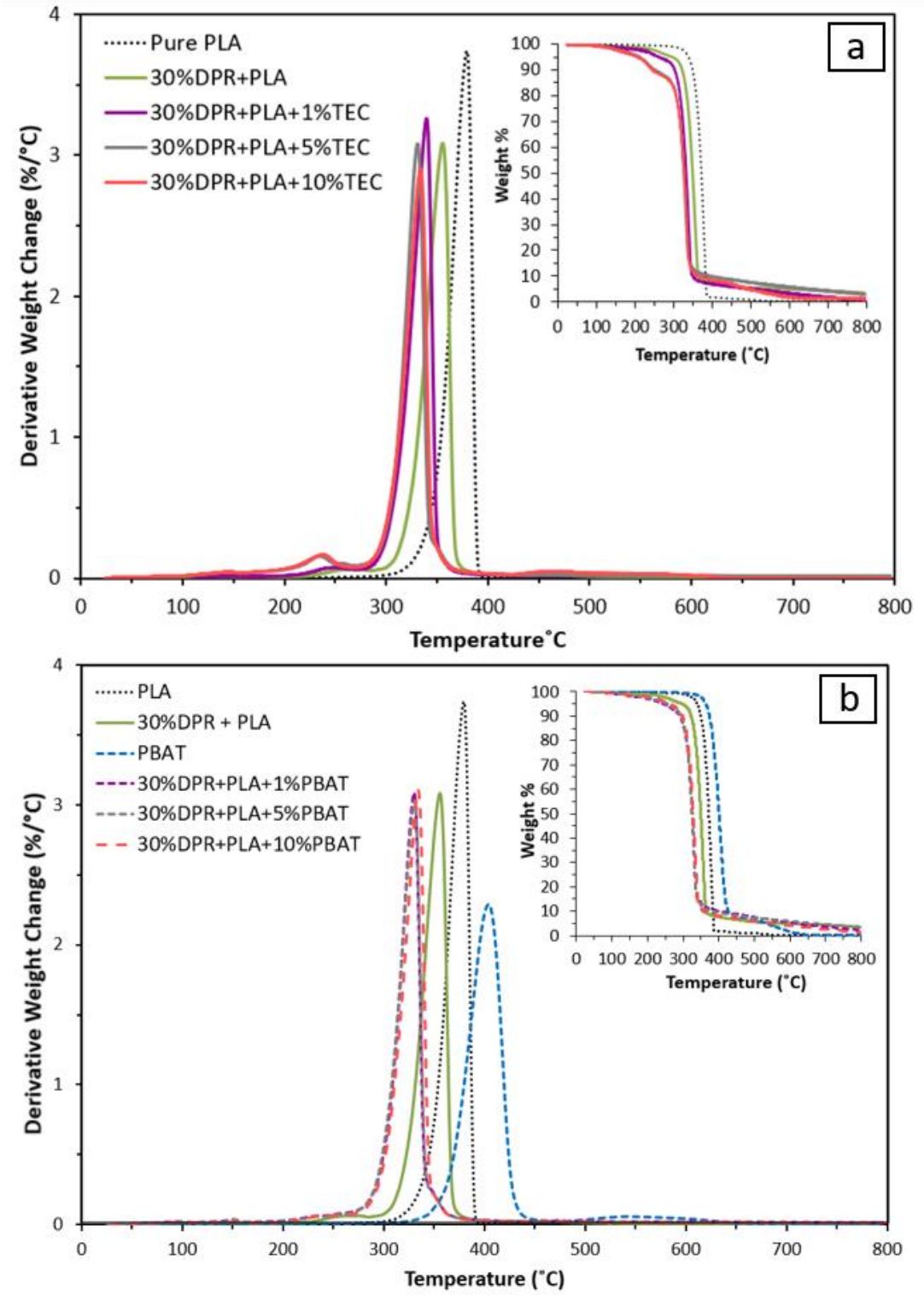

Figure 36: Derivative weight change and TGA plots of the plasticized 30% DPR-PLA composites with three levels of (a) TEC and (b) PBAT.

3.2.2 Differential Scanning Calorimetry (DSC)

The glass transition temperatures (T_g) of the plasticized 30% DPR-PLA composites with TEC and PBAT were obtained from the second heating of the DSC curves and presented in Figure 37. The T_g of the 30% DPR-PLA composite shows insignificant reduction with the addition of 1 wt% PBAT, then it remains constant with increasing PBAT content (Figure 37 (a)). Similar observations were attained by [125]. The glass transition temperatures of the 30% DPR-PLA composite shifts to lower temperatures with increasing TEC content and it diminishes by the addition of 10 wt% TEC (Figure 37 (b)). The reduction is due to the increase in the plasticizing effect of the low molecular weight TEC, which occupies intermolecular spaces and leads to poor interaction between PLA, DPR filler and TEC. This will probably increase the polymer molecular mobility, which in turn reduces the glass transition temperatures [95]. Analogous reduction in glass transition temperatures was observed for PLA and Chitin nanocrystal nanocomposites with increasing TEC content by [126].

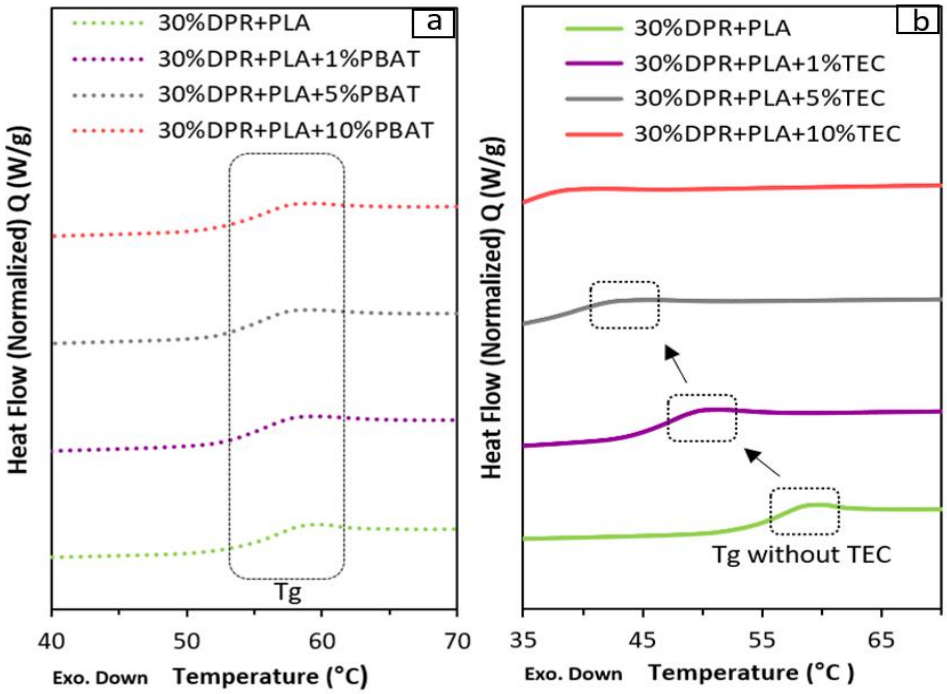

Figure 37: The glass transition temperatures (T_g) from DSC thermograms of the plasticized 30% DPR-PLA with (a) PBAT and (b) TEC.

3.2.3 Fourier Transforms Infrared Spectroscopy (FTIR)

The interaction identification after the addition of three levels of two plasticizers (TEC & PBAT) to 30% DPR-PLA composite was investigated with FTIR. The infrared spectrum obtained after the incorporation of the first plasticizer (TEC) is shown in Figure 38. The main differences are linked to fingerprint region from 1850 cm^{-1} to 600 cm^{-1}. In the plasticized composites with TEC, low intensity peaks were observed between 3660 and 3475 cm^{-1} due to –OH stretching. A slight increase in the intensity of the bands observed at 2916.32 cm^{-1} and 2848.35 cm^{-1} that attributed to the stretching of C—H in CH_3 was seen with increasing TEC content. In Figure 38, all composites displayed a sharp peak at 1751 cm^{-1} that attributes to the distinctive carbonyl peak in the PLA chemical structure. The –C=O peak intensity of 30% DPR-PLA composite raised sharply by the addition of 1 wt% TEC. Then it shifted slightly

from 1751.4 cm^{-1} to 1748.8 cm^{-1} with increasing TEC content to 10 wt%. A similar increasing behavior in intensity was observed at 1180.704 cm^{-1} due to the -CH-O- group (–C-O- stretching bond). Also, similar behavior is displayed at the three distinctive peaks 1128.153, 1081.870 and 1039.444 cm^{-1} as shown in Figure 38. These findings agree with the research work conducted on PLA based composites with 10 wt% TEC [127].

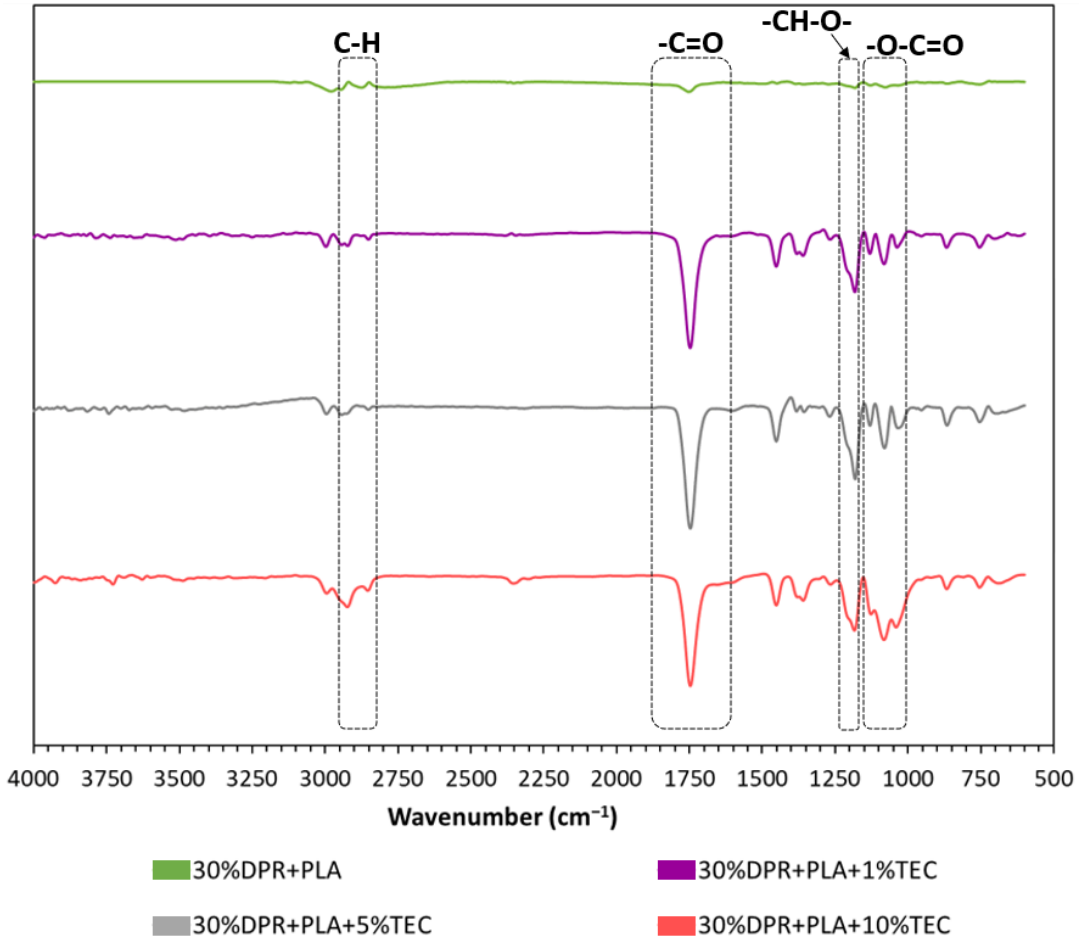

Figure 38: FTIR spectra of the plasticized 30% DPR-PLA with TEC.

The FTIR spectra of PBAT and the plasticized 30% DPR-PLA composites using PBAT are presented in Figure 39. The peaks at about 2945.5 cm^{-1} resulted from the vibrations of C–H indicating the existence of alkyl chains. The PBAT spectrum

clearly shows sharp intense peaks at 1750 cm^{-1} corresponding to the –C=O groups. The intensity of –C=O peak of 30% DPR-PLA composite increased sharply by the addition of 1 wt% PBAT, then it gradually decreased with increasing PBAT content. For pure PBAT and the plasticized composites with PBAT, antisymmetric C-O-C stretching vibration bonds were observed at 1250 cm^{-1}. Since the DPR was held at 30 wt% in the three plasticized composites, no significant changes, and no considerable chemical interactions between PLA and PBAT were noticed. The only changes were in the sudden increase in the relative transmittance (%) after the incorporation of 1 wt% PBAT. This finding was confirmed when referring to the identical PLA glass transition temperatures in the three plasticized composites with PBAT (Figure 37(a)), indicating immiscibility between PLA and PBAT. Similar results were observed in the literature during the fabrication of (PLA-Babassu-PBAT) films for mulch application [128].

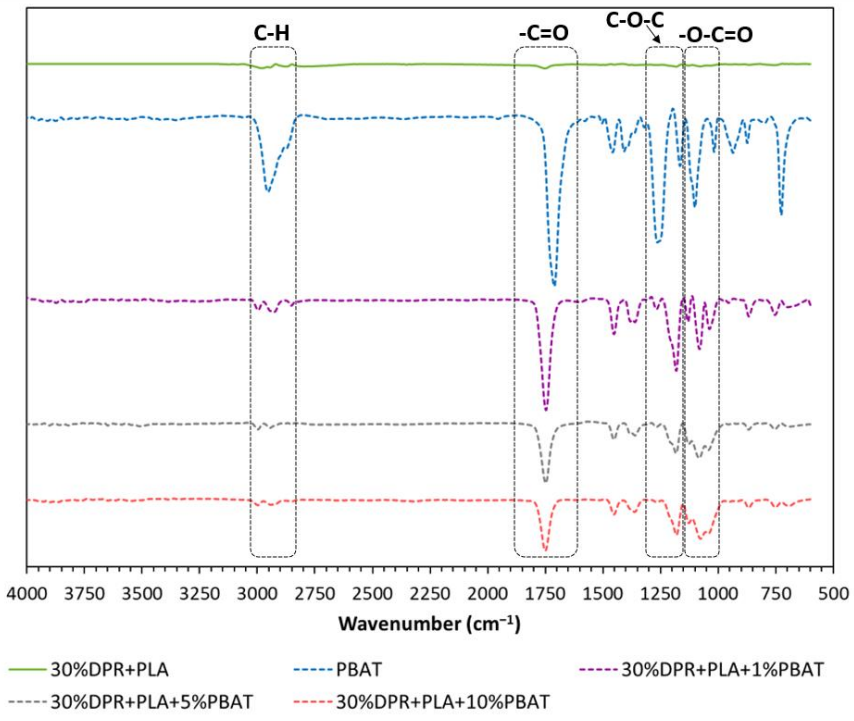

Figure 39: FTIR spectra of the plasticized 30% DPR-PLA with PBAT.

3.2.4 Scanning Electron Microscopy (SEM)

Scanning Electron Microscopy (SEM) analysis was used to observe the surface morphology of the plasticized 30% DPR-PLA composites fracture surfaces after tensile testing. SEM was used to investigate the effect of the addition of 1 wt% and 10 wt% of two plasticizers (TEC and PBAT) on the morphology and phase adhesion of the composite. Figure 40(a) shows the micrograph of PBAT resin, presenting ductile fracture with higher continuous smooth phase compared with neat PLA (Figure 40(b)). Analogous SEM images were observed for PLA and PLA-PBAT by [114].

The addition of 1 wt% TEC (Figure 40(d)) shows slightly higher biomass coverage when compared to the plasticized 30% DPR-PLA composite with 1 wt% PBAT (Figure 40(c)). However, the incorporation of 10 wt% PBAT in the 30% DPR-PLA composite resulted in a smooth surface and exhibited well-dispersed biomass in the PLA matrix as shown in Figure 40(e). Also, some PBAT presence of less than 5 μm in size was observed in the PLA matrix, which might be due to the transesterification reaction between PBAT and PLA. A high co-continuous phase and adhesion might be formed between the two phases at higher composition of PBAT [125]. Moreover, the addition of 10 wt% of TEC in Figure 40(f) enhanced the dispersion of the biomass in the composite and reduced large agglomeration of the biomass filler. Similar observation of well-dispersed chitin nanocrystals in the PLA matrix after the use of about 7.5 wt% TEC was reported [126].

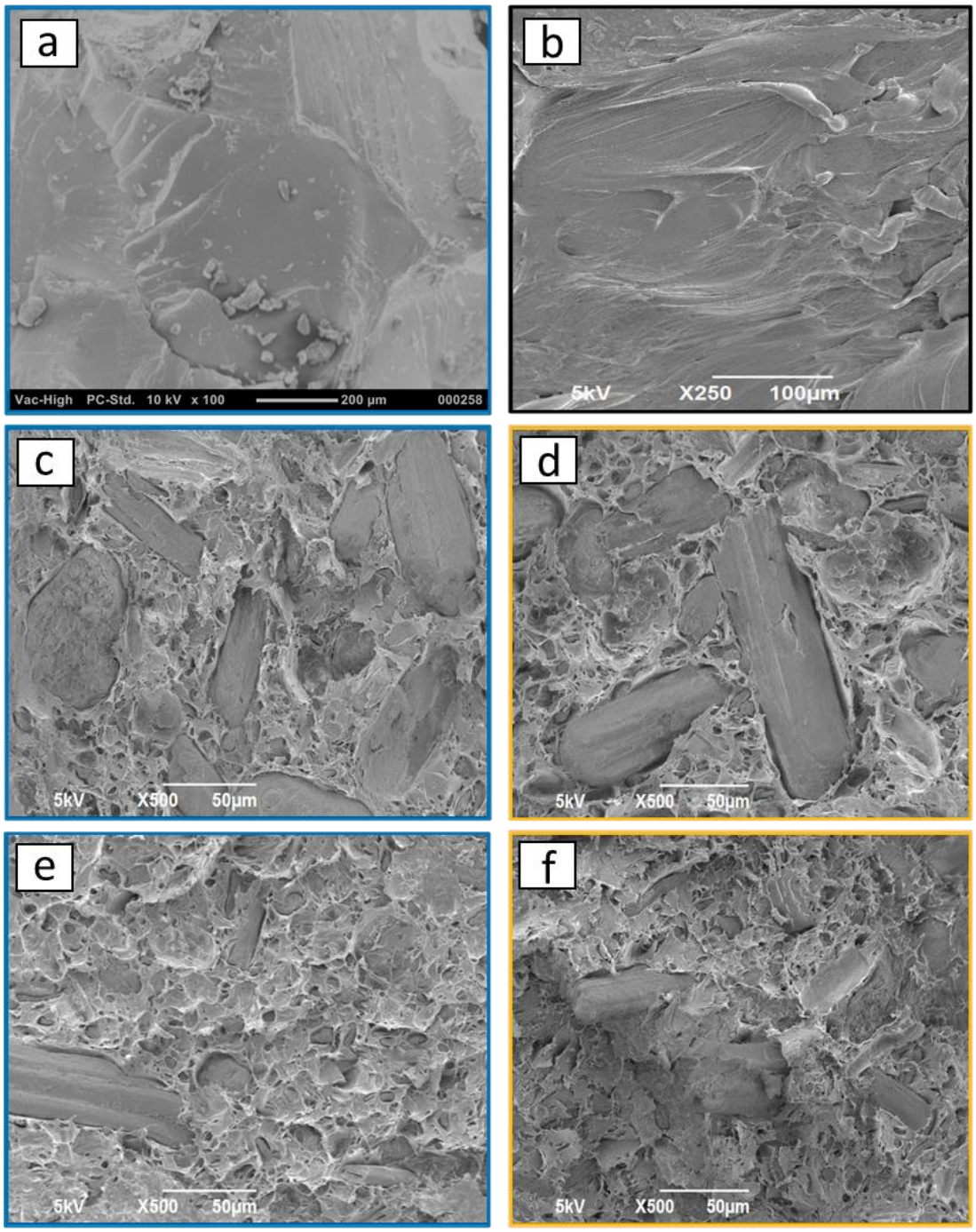

Figure 40: SEM images of (a) pure PBAT, (b) pure PLA, (c) 30% DPR (90 µm)+PLA+1% PBAT, (d) 30% DPR (90 µm)+PLA+1% TEC, (e) 30% DPR (90 µm)+PLA+10% PBAT, (f) 30% DPR (90 µm)+PLA+10% TEC.

3.2.5 Tensile strength

A polymer matrix is generally designated to be suitable for a specific form of natural fiber. The date palm fiber (DPF) has the highest tensile strength compared with other frequently used fibers such as bamboo, sisal, and coir. This is due to the high cellulose content of the DPF [69]. PLA is considered as one of the relatively brittle biodegradable polymers with an acceptable tensile strength to be used in packaging and medical applications. Biodegradable plasticizers such as Triethyl Citrate (TEC) and Polybutylene Adipate-co-Terephthalate (PBAT) are utilized to enhance PLA ductility, flexibility, and processability. But this will be done at the expense of the reinforcing feasibility and tensile strength. Mechanical tests were performed for PLA and 30% DPR-PLA composites to demonstrate the effect of the addition of three levels of two plasticizers (TEC and PBAT) on the mechanical properties of the composite material.

Figure 41 shows that the tensile strength of pure Polylactic Acid (PLA 2003D) is 68.88 MPa, which agrees with other researchers' findings [129]. The incorporation of 30 wt% of DPR filler clearly decreased the tensile strength of the PLA by 46% as shown in Figure 41. This significant decrease can be explained by the development of biomass agglomerates, micro-voids, and porosity during the composite fabrication. Therefore, these developments in the PLA matrix will minimize the reinforcing feasibility of the DPR filler for carrying such applied stress. The tensile strength is improved from 31.82 MPa to 46.49 MPa by the addition of 1 wt% Triethyl Citrate (TEC) to the 30% DPR-PLA composite during fabrication. A clear decrease by more than 10 MPa in tensile strength is observed by further increase in the TEC composition up to 10 wt%.

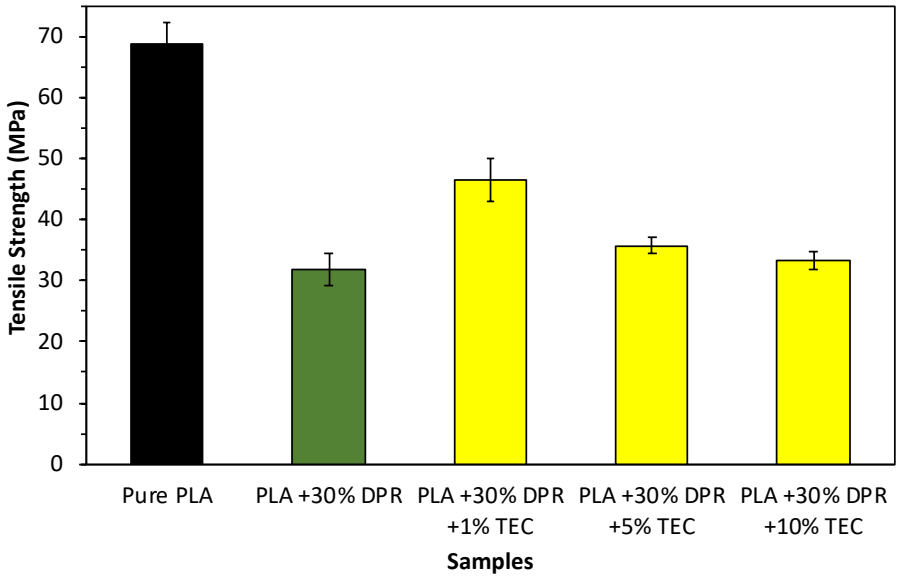

Figure 41: The tensile strength of PLA and its 30% DPR -PLA composites with three levels of TEC (1 wt%, 5 wt%, 10 wt%).

The addition of 1 wt% PBAT to the 30% DPR-PLA composite as an alternative plasticizer to TEC increased the tensile strength from 31.82 MPa to 43.65 MPa as displayed in Figure 42. A minimal decrease in the tensile strength to 39.06 MPa was noticed by the addition of 5 wt% PBAT. A significant reduction in tensile strength to 21.80 MPa was noticed by the incorporation of 10 wt% PBAT to the 30% DPR-PLA composite. This reduction was predicted due to the low tensile strength of the PBAT (21 MPa) compared to that of pure PLA [130].

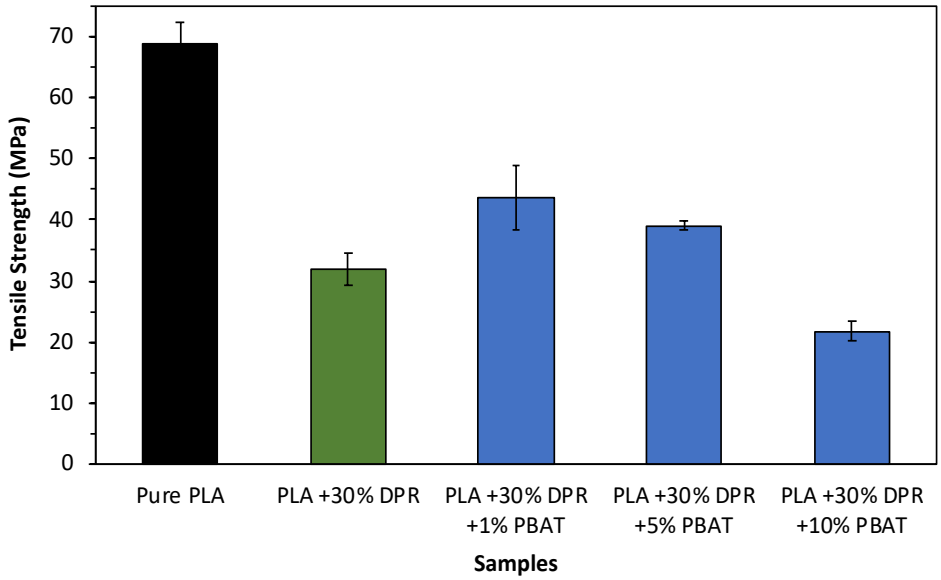

Figure 42: The tensile strength of PLA and its 30% DPR-PLA composites with three levels of PBAT (1 wt%, 5 wt%, 10 wt%).

Figure 43 displays the tensile strength of the plasticized 30% DPR-PLA composites with the three levels of TEC compared with PBAT as an alternative plasticizer. As expected, both plasticizers enhanced the tensile strength of 30% DPR-PLA composite at lower composition. A similar decreasing trend in the tensile strength is noticed by the addition of 10 wt% from the two plasticizers. The addition of 1 wt% and 5 wt% of both plasticizers to the 30% DPR-PLA showed a similar effect on the tensile strength. The incorporation of 10 wt% PBAT showed a much lower tensile strength (21.80 MPa) compared to 10% TEC (33.20 MPa).

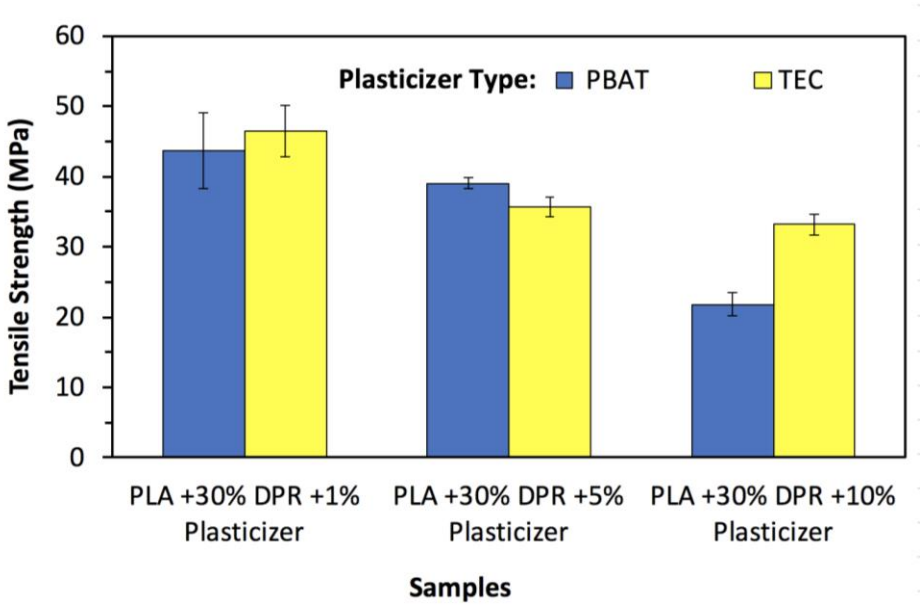

Figure 43: The tensile strength of 30% DPR-PLA composites with three levels of two plasticizers.

3.2.6 Elongation at break

The elongation at break of PLA (2003D) as a rough and brittle polyester is 5% as shown in Figure 44. This agrees with the research work that is investigated by [131]. The addition of 30 wt% of DPR (90 µm) caused a significant decrease in the elongation at break to 1.80%. This is because of the absence of a total random uniform distribution of DPR in the PLA matrix, resulting in higher tendency of the bio-composite to break. Other researchers have demonstrated a decline in elongation at break as well with the increase in natural filler [132]. The 30% DPR-PLA composite needs to be plasticized to overcome rigidness and brittleness challenges. The results revealed that the 30% DPR-PLA composite's ductility could be enhanced by incorporating just 1 wt% TEC, which improved the elongation at break from 1.80% to 3.23%. A minimal increase to 3.48% in elongation at break of the 30% DPR-PLA composite was observed by the

addition of 5 wt% TEC while the elongation increased to 4.20% when 10 wt% TEC was used.

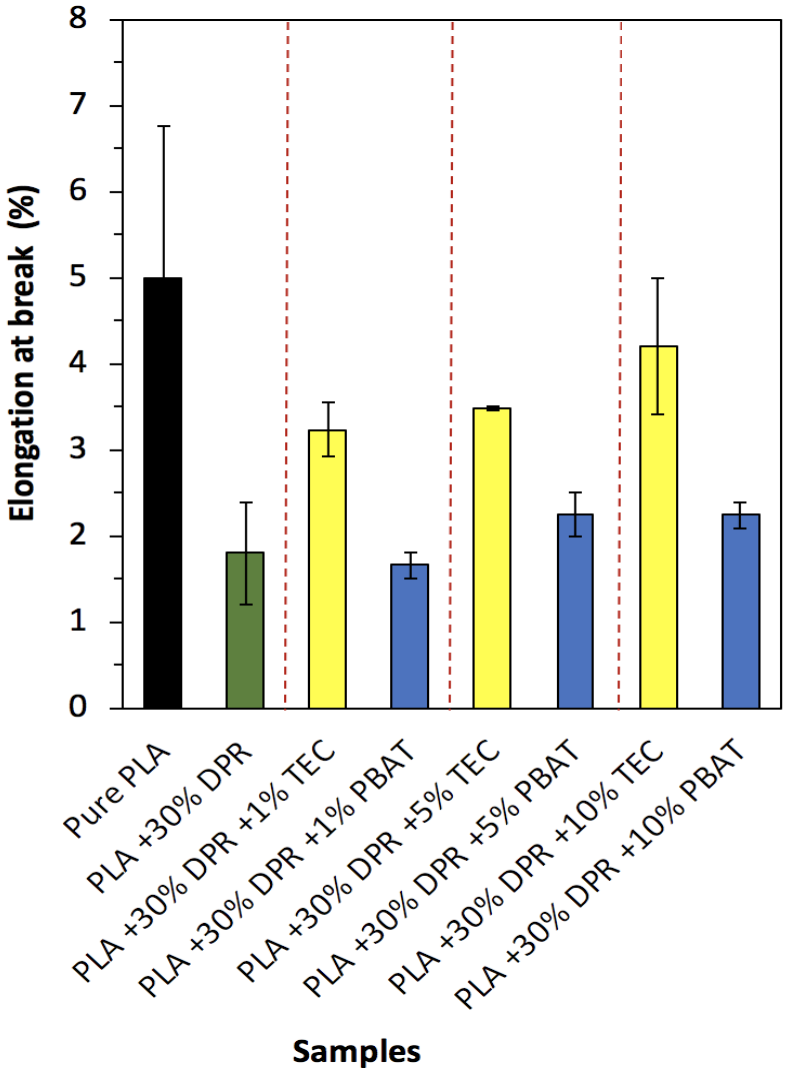

Figure 44: The elongation at break of PLA and its 30% DPR-PLA composites with three levels of two plasticizers (TEC and PBAT).

On the other hand, the addition of 1 wt% PBAT showed relatively no effect regarding the elongation at break of the 30% DPR-PLA composite as displayed in Figure 44. However, the elongation at break enhanced to 2.25% after the addition of 5 wt% PBAT and remained the same even by increasing the plasticizer to 10 wt% PBAT.

Deng and co-author showed a significant increase in the elongation at break above 10 wt% PBAT with different zones and possible mechanism for different ranges of PBAT content [133]. The results for up to 10% plasticizer proved the superior effect of TEC compared with PBAT in terms of improving the elongation at break of the 30% DPR-PLA composite as shown in Figure 44. This might be due to the penetration of TEC molecules within the interface between the PLA and the granules of biomass, thus reducing the binding force, and making it possible for molecular chains to move and slip, thereby enhancing the elongation [134].

3.2.7 Water absorption behavior

The key drawback of natural fiber reinforced polymers is their hydrophilic nature which is highly responsive to water. This limitation affects their physical, thermal, and mechanical performance. Water absorption tests were carried out for DPR-PLA optimum composite in seawater (37 ppt) and tap water at room temperature for 2500 hours immersion while hot water immersion was done at 50°C for 48 hours. Figure 45 represents the water retention percentage versus soaking time in seawater, tap water and hot water for the first 24 hours. The maximum water absorption of 9.34 wt% was attained for the hot water after 24 hours. The same composite absorbs water in a lower rate in the first 24 hours of soaking in room temperature tap water, and seawater with a water retention percentage of 1.48 wt% and 0.25 wt%, respectively. Also, the most color fade off after 48 hours was observed for the hot water as shown in Figure 46.

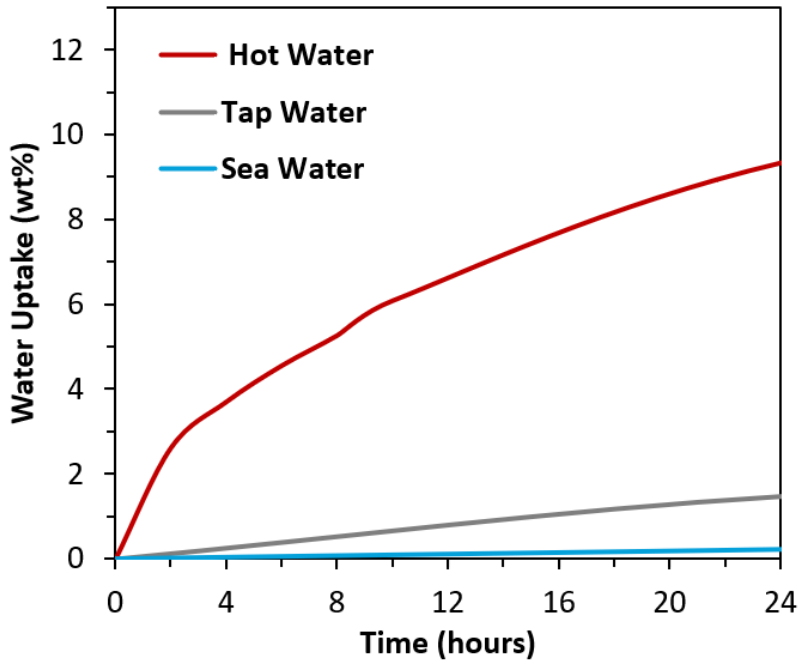

Figure 45: Water retention (wt%) versus soaking time of 30% DPR-PLA samples in hot water, tap water and seawater for the first 24 hours.

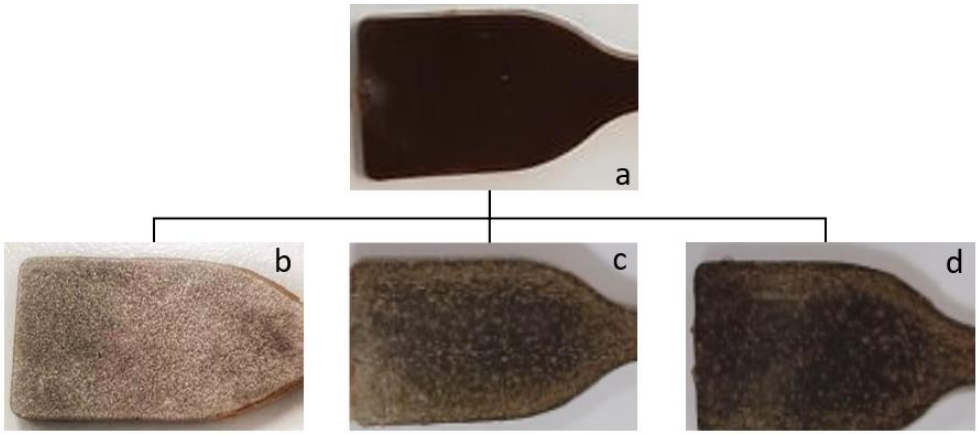

Figure 46: Change of the color of (a) 30% DPR-PLA specimen after soaking in (b) hot water (50°C), (c) tap water and (d) saline water after 48 hours.

The water uptake curves of 30% DPR-PLA specimens that were immersed in in hot water, tap water and seawater are shown in Figure 47. The major water uptake was 12.00 wt% after 48 hours of immersion in hot water. In both tap water and seawater, the water uptake of the specimens increased with the immersion time at early

stage to reach a maximum of 2.68 wt%, and 1.83 wt%, respectively. Then it fluctuated until it reached a water absorption of 1.80 wt% and 0.039 wt% after 2500 hours of immersion in tap water and seawater, respectively. A group of researchers found that the water absorption by PLA (2003D) in tap water was up to 1 wt% after 50 days and achieved a point of equilibrium, where the weight of the PLA sample remained constant [45]. Then they observed that the water uptake increased with the addition of cellulose from durian rinds compared with pure PLA, due to the rise of hydroxyl groups in the PLA based composite [135]. On the other hand, non-biodegradable cutlery from pure Polystyrene available in market showed water absorption of 0.03–0.1 wt%, which is lower by 10% compared with PLA [44].

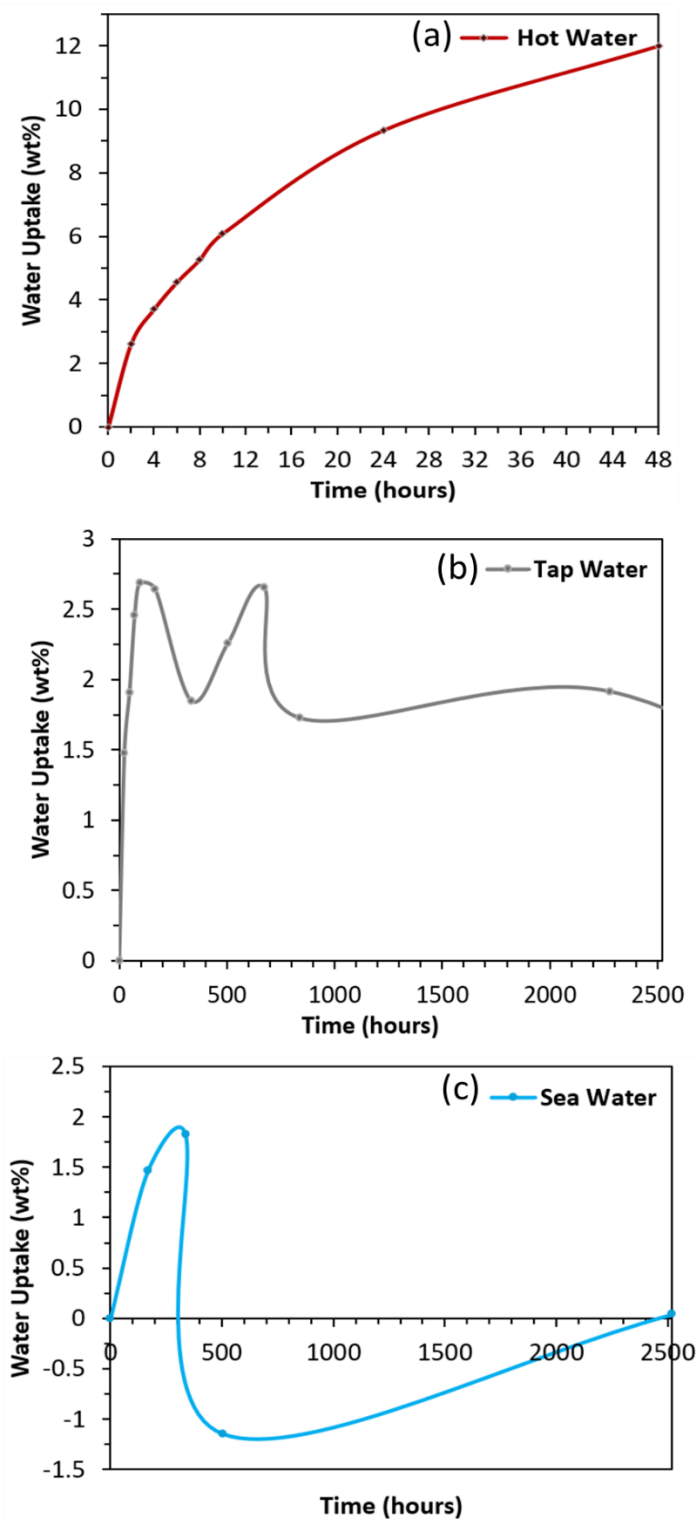

Figure 47: Water uptake (wt%) versus soaking time of 30% DPR-PLA composite in (a) hot water, (b) tap water, and (c) sea water.

Figure 47 also shows that the overall water absorption for 30% DPR-PLA composites immersed in tap water is higher than those immersed in seawater with a

slight noticeable color change in the water. This is because of the presence of salt molecules in the seawater which decreases the activity of H_2O molecules. The partial coverage of the surface of the specimen by salt molecules can inhibit water uptake [136]. Another observation was the loss of the sample original weight by more than 1 wt% in seawater immersion at the first 300 hours (12.5 days). A group of researchers suggested that the hydrolysis of cellulose within the biomass may favors the seawater [137].

3.2.8 Biodegradability test

The percentage weight loss of PLA based composites and commercial samples, which were buried in soil were recorded after 4 months and the final appearance are shown in Figure 48. The burial was done at 5 cm and 22 cm depth of dry and watered soil. It can be seen from Figure 48 that the size of all bio-composite samples become smaller (up to 3.06% weight loss) with a burial time of 4 months compared with 0.15% weight loss for the commercial samples. This is attributed to the digestion of the samples by the microorganisms such as bacteria and fungi. After 4 months, 30% DPR-PLA samples lost their integrated appearance, illustrating that their degradation speed is faster than those of 15% DPR-PLA samples. All samples that were placed at soil depth of 22 cm had their original color fade more than those placed 5 cm deep from the top of the bucket.

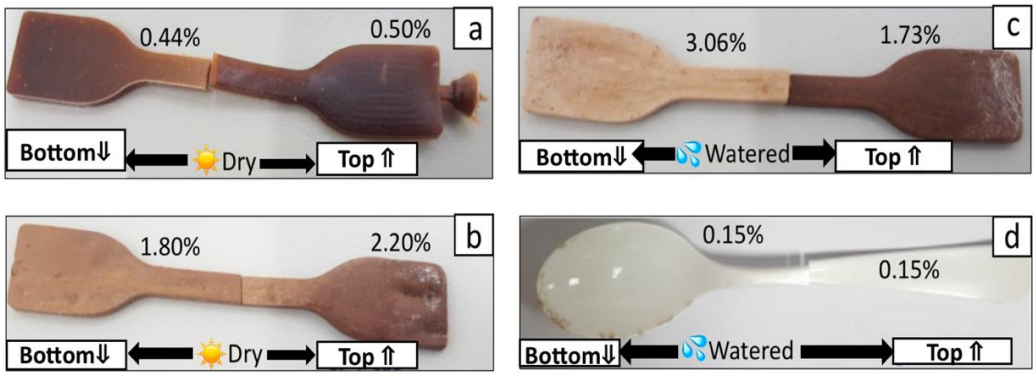

Figure 48: Percentage weight loss after 4 months burial of (a) 15% DPR-PLA in dry soil, (b) 30% DPR-PLA in dry soil, (c) 30% DPR-PLA composites in watered soil, and (d) commercial samples in watered soil at two heights.

The anaerobic conditions of soil at 22 cm soil depth were more favorable for the biodegradation of PLA-based samples that were watered. The 30% DPR-PLA sample that was placed in the bottom watered soil had most color fade off with a weight loss of 3.06%. This observation indicates that watered soil favors faster degradation when compared with dry soil. But the case was different when comparing the weight loss of 30% DPR-PLA samples at the top of the bucket in dry soil with that of watered soil as shown in Figure 48 (b) and Figure 48 (c), respectively. The weight loss was slightly higher and the sample surface was rougher in the case of the sample placed in the top region of the dry soil, which could be due to the erosion effects as reported by [138].

Chapter 4: Conclusion

In this study, the new green composite material was developed from Polylactic Acid (PLA) mixed with 30%, 40%, and 50% by weight rachis biomass from UAE date palm waste (DPR) for cutlery and food ware applications. The DPR was used without any chemical treatments or surface modification to avoid the use of chemicals in food-grade applications, save energy and reduce production cost. Melt mixing was performed at 180°C followed by the extrusion of DPR-PLA composites, which were then re-melted via Injection Molding machine to fill the closed mold cavity of a certain shape. The prepared DPR-PLA composites were subjected to different thermal, mechanical, and physical tests.

To prevent possible thermal degradation during processing, TGA revealed that the weight loss of five percent of PLA occurs at about 338.9°C while the DPR biomass demonstrates a five percent weight loss at approximately 206.3°C. The DPR biomass had good thermal stability by showing a final residue of 23 wt% at 800°C. The bio-composites of PLA with a biomass content of 30%, 40%, and 50% by weight showed degradation temperatures of 355.8°C, 346.8°C, and 335.9°C, respectively. The glass transition temperature of PLA was obtained to be 59.13°C while the glass transition temperature of DPR-PLA composites shifts to slightly lower temperatures (54.1°C) with a filler content of 50% by weight, thereby improving the ductility and processability of the PLA.

FTIR results indicated potential interfacial interaction between PLA and DPR biomass. One of the changes could be the esterification reaction between –OH of the biomass, the carbonyl (C=O), and the terminal –COOH group in the PLA, causing a gradual increase in the intensity of the C=O stretching peak, when the biomass was

increased in the composite sample. Moreover, SEM results indicated that the DPR is in particulate form, which appears as aggregates of some nanofibrils on the surfaces of the biomass particles. Similar uniform dispersion of the filler with the particle size of 53 μm and 90 μm in the PLA matrix was observed by the addition of 30 wt% biomass. The addition of 40 wt% and 50 wt% biomass filler made the surface slightly rougher and coarser when compared with 30% DPR-PLA composites.

The MFI of PLA was measured to be 7.05g/10 min, while the addition of 50 wt% DPR to the PLA, increased the MFI to 54.78g/10 min, which might be due to the increase in the mobility of the PLA chain and the reduction of composite viscosity. The 30% DPR-PLA composite was considered as the optimum composite composition for processing in large scale extruders due to its lower MFI (16 g/10 min) when compared to the other bio-composites. The tensile strengths of pure PLA (2003D) and 30% DPR-PLA composite was found to be 68.88 MPa and 31.82 MPa, respectively. The incorporation of 10 wt% PBAT showed much lower tensile strength (21.80 MPa) compared with that of 10 wt% TEC (33.20 MPa). Finally, the results proved the superior effect of 10 wt% TEC in terms of improving the elongation at break of the 30% DPR-PLA composite from 1.8% to 4.20%.

A maximum water absorption of 9.34 wt% was obtained after soaking the optimum 30% DPR-PLA composite in hot water after 24 hours of immersion. The same composite in the first 24 hours of soaking in room temperature tap water, and seawater showed a water absorption of 1.48 wt% and 0.25 wt%, respectively. In addition, the 30% DPR-PLA sample that was placed in the bottom of the watered soil had most color fade off with the highest weight loss percentage of 3.06% after 4 months. The industrial composting is expected to be much faster (around 6 to 12 weeks) due to the more favorable biodegradability conditions.

To sum up, this green composite will play an essential role in decreasing the environmental concerns caused by the land and ocean pollution from petroleum-based plastics and their serious consequences. This research focused on developing a biodegradable composite material made from date palm waste to replace single-use cutlery plastics used in homes, parks, restaurants, coffee shops, and air flights. The optimum plasticized 30% DPR-PLA composite is believed to be suitable for cutlery application since it showed comparable properties to petroleum-based plastics especially in terms of tensile strength, elongation at break, and cost as shown in Table 2. The main limitation of the DPR-PLA composite is its slightly hydrophilic nature, which is more responsive to water compared to petroleum-based plastics.

For future work, a group of food-grade biodegradable plasticizers and other additives (compatibilizer, anti-caking, and antioxidant agent) are recommended to be studied in the formula in order to optimize the final composite characteristics in terms of tensile strength, flexural strength, Melt Flow Index, and cost. Also, the determination of the crystallographic structure using XRD (X-Ray Diffraction) analysis will be useful in dictating the mold-opening time versus the economics of the whole process. However, this study can target different applications such as straws, food packaging, iceboxes, and insulated containers by varying the processing techniques, composite formula, and conducting the required testing. Furthermore, it is recommended to develop a real composting soil system similar to the industrial one with controlled humidity, temperature (50–70°C) and type and number of microbes to study the rate of degradation and check the rate of production of CO_2, water, CH_4, biomass, and other natural substances.

References

[1] A. N. Frone, S. Berlioz, J.-F. Chailan, and D. M. Panaitescu, 'Morphology and thermal properties of PLA–cellulose nanofibers composites', *Carbohydr. Polym.*, vol. 91, no. 1, pp. 377–384, 2013. doi:10.1016/j.carbpol.2012.08.054

[2] R. Chandra and R. Rustgi, 'Biodegradable polymers', *Prog. Polym. Sci.*, vol. 23, no. 7, pp. 1273–1335, 1998. doi:10.1016/s0079-6700(97)00039-7

[3] Waste and Recycling Middle East and Africa, 'UAE date palm tree owners to receive cash for palm waste'. https://www.wasterecyclingmea.com/uae-date-palm-tree-owners-to-receive-cash-for-palm-waste/ (accessed Dec. 25, 2020).

[4] D. Klemm, B. Heublein, H.-P. Fink, and A. Bohn, 'Cellulose: fascinating biopolymer and sustainable raw material', *Angew. Chem. Int. Ed.*, vol. 44, no. 22, pp. 3358–3393, 2005. doi:10.1002/anie.200460587

[5] H. Ritchie and M. Roser, 'Plastic pollution', *Our World Data*, Sep. 2018. https://ourworldindata.org/plastic-pollution (accessed Dec. 25, 2020).

[6] M. McMahon, 'What is dent corn? (with pictures)', *Delighted Cooking*. http://www.delightedcooking.com/what-is-dent-corn.htm (accessed Dec. 25, 2020).

[7] USDA, 'BioPreferred'. https://www.biopreferred.gov/BioPreferred/faces/Welcome.xhtml (accessed Dec. 25, 2020).

[8] R. C. Thompson, S. H. Swan, C. J. Moore, and S. Frederick, 'Our plastic age.', *Philos. Trans. R. Soc. B Biol. Sci.*, vol. 364, no. 1526, pp. 1973–1976, 2009. doi:10.1098/rstb.2009.0054

[9] S. Reddy, 'Preventing ocean plastics'. https://pew.org/2OGFDWG (accessed Dec. 25, 2020).

[10] R. Kavlock *et al.*, 'phthalates expert panel report on the reproductive and developmental toxicity of di (2-ethylhexyl) phthalate', *Reprod Toxicol*, vol. 16, pp. 529–653, 2002. doi:10.1016/s0890-6238(02)00032-1

[11] A. Grover, A. Gupta, S. Chandra, A. Kumari, and S. M. Khurana, 'Polythene and environment', *Int. J. Environ. Sci.*, vol. 5, no. 6, pp. 1091–1105, 2015. doi: 10.6088/ijes.2014050100103

[12] G. Caruso, 'Plastic degrading microorganisms as a tool for bioremediation of plastic contamination in aquatic environments', *J Pollut Eff Cont*, vol. 3, no. 3, pp. 1–2, 2015. doi: 10.4172/2375-4397.1000e112

[13] R. E. Conn *et al.*, ‘Safety assessment of polylactide (PLA) for use as a food-contact polymer’, *Food Chem. Toxicol.*, vol. 33, no. 4, pp. 273–283, 1995. doi:10.1016/0278-6915(94)00145-e

[14] K. Marsh and B. Bugusu, ‘Food packaging—roles, materials, and environmental issues’, *J. Food Sci.*, vol. 72, no. 3, pp. R39–R55, 2007.

[15] Earth Institute, ‘The truth about bioplastics’, *State of the Planet*, Dec. 13, 2017. https://blogs.ei.columbia.edu/2017/12/13/the-truth-about-bioplastics/ (accessed Dec. 25, 2020).

[16] P. H. Yu, H. Chua, A. L. Huang, W. Lo, and G. Q. Chen, ‘Conversion of food industrial wastes into bioplastics’, *Appl. Biochem. Biotechnol.*, vol. 70, no. 1, pp. 603–614, 1998. doi:10.1007/bf02920172

[17] T. M. Letcher, ‘Introduction to plastic waste and recycling’, *Plastic Waste and Recycling*, Elsevier, 2020, pp. 3–12. doi:10.1016/B978-0-12-817880-5.00001-3

[18] Y. Zhong, P. Godwin, Y. Jin, and H. Xiao, ‘Biodegradable polymers and green-based antimicrobial packaging materials: A mini-review’, *Adv. Ind. Eng. Polym. Res.*, vol. 3, no. 1, pp. 27–35, 2020. doi:10.1016/j.aiepr.2019.11.002

[19] M. Van den Oever, K. Molenveld, M. van der Zee, and H. Bos, *Bio-based and biodegradable plastics: facts and figures: focus on food packaging in the Netherlands*, no. 1722. Wageningen Food & Biobased Research, 2017. doi: 10.18174/408350

[20] M. G. L. Ramírez, K. G. Satyanarayana, S. Iwakiri, G. B. de Muniz, V. Tanobe, and T. S. Flores-Sahagun, ‘Study of the properties of biocomposites. Part I. Cassava starch-green coir fibers from Brazil’, *Carbohydr. Polym.*, vol. 86, no. 4, pp. 1712–1722, 2011. doi:10.1016/j.carbpol.2011.07.002

[21] C. J. Weber, V. Haugaard, R. Festersen, and G. Bertelsen, ‘Production and applications of biobased packaging materials for the food industry’, *Food Addit. Contam.*, vol. 19, no. S1, pp. 172–177, 2002. doi:10.1080/02652030110087483

[22] F. S. Isotton, G. L. Bernardo, C. Baldasso, L. M. Rosa, and M. Zeni, ‘The plasticizer effect on preparation and properties of etherified corn starchs films’, *Ind. Crops Prod.*, vol. 76, pp. 717–724, 2015. doi: 10.1016/j.indcrop.2015.04.005

[23] M. N. Abdorreza, L. H. Cheng, and A. A. Karim, ‘Effects of plasticizers on thermal properties and heat sealability of sago starch films’, *Food Hydrocoll.*, vol. 25, no. 1, pp. 56–60, 2011. doi: 10.1016/j.foodhyd.2010.05.005

[24] J.-Y. Chee, S.-S. Yoga, N.-S. Lau, S.-C. Ling, R. M. Abed, and K. Sudesh, ‘Bacterially produced polyhydroxyalkanoate (PHA): converting renewable resources into bioplastics’, *Curr. Res. Technol. Educ. Top. Appl. Microbiol. Microb. Biotechnol.*, vol. 2, pp. 1395–1404, 2010.

[25] E. L. Bradley, A. House, J. S. Day, M. Driffield, and S. Hutton, ‘Biobased materials used in food contact applications: an assessment of the migration potential’, *Rep. FD*, vol. 10, no. 04, 2010.

[26] A. Ivonkovic, K. Zeljko, S. Talic, and M. Lasic, ‘Biodegradable packaging in the food industry’, *J. Food Saf. Food Qual.*, vol. 68, pp. 26–38, 2017. doi: 10.2376/0003-925X-68-26

[27] R. M. Rasal, A. V. Janorkar, and D. E. Hirt, ‘Poly (lactic acid) modifications’, *Prog. Polym. Sci.*, vol. 35, no. 3, pp. 338–356, 2010. doi:10.1016/j.progpolymsci.2009.12.003

[28] R. N. Tharanathan, ‘Biodegradable films and composite coatings: past, present and future’, *Trends Food Sci. Technol.*, vol. 14, no. 3, pp. 71–78, 2003. doi:10.1016/s0924-2244(02)00280-7

[29] A. A. Shah, F. Hasan, A. Hameed, and S. Ahmed, ‘Biological degradation of plastics: a comprehensive review’, *Biotechnol. Adv.*, vol. 26, no. 3, pp. 246–265, 2008. doi: 10.1016/j.biotechadv.2007.12.005

[30] C. Maraveas, ‘Environmental sustainability of greenhouse covering materials’, *Sustainability*, vol. 11, no. 21, p. 6129, 2019. doi: 10.3390/su11216129

[31] V. Katiyar, *Bio-based Plastics for Food Packaging Applications*. Smithers Pira, 2017.

[32] C. R. Reshmi, S. P. Sundaran, A. Juraij, and S. Athiyanathil, ‘Fabrication of superhydrophobic polycaprolactone/beeswax electrospun membranes for high-efficiency oil/water separation’, *RSC Adv.*, vol. 7, no. 4, pp. 2092–2102, 2017. doi:10.1039/C6RA26123J

[33] R. M. da S. M. Thiré, L. C. Arruda, and L. S. Barreto, ‘Morphology and thermal properties of poly (3-hydroxybutyrate-co-3-hydroxyvalerate)/attapulgite nanocomposites’, *Mater. Res.*, vol. 14, no. 3, pp. 340–344, 2011. doi:10.1590/S1516-14392011005000046

[34] J. Shah and M. R. Jan, ‘Effect of polyethylene terephthalate on the catalytic pyrolysis of polystyrene: Investigation of the liquid products’, *J. Taiwan Inst. Chem. Eng.*, vol. 51, pp. 96–102, 2015. doi:10.1016/j.jtice.2015.01.015

[35] T. F. Cipriano, A. L. N. da Silva, A. H. M. da F. T. da Silva, A. M. F. de Sousa, G. M. da Silva, and M. G. Rocha, ‘Thermal, rheological and morphological properties of poly (lactic acid)(PLA) and talc composites’, Polímeros, vol. 24, no. 3, pp. 276–282, 2014. doi:10.4322/polimeros.2014.067

[36] J. P. Mofokeng and A. S. Luyt, 'Morphology and thermal degradation studies of melt-mixed poly (hydroxybutyrate-co-valerate)(PHBV)/poly (ε-caprolactone)(PCL) biodegradable polymer blend nanocomposites with TiO 2 as filler', *J. Mater. Sci.*, vol. 50, no. 10, pp. 3812–3824, 2015. doi: 10.1007/s10853-015-8950-z

[37] M. C. G. Rocha and L. R. da C. Moraes, 'Low density polyethylene (LDPE) blends based on poly (3-hydroxi-butyrate) (PHB) and guar gum (GG) biodegradable polymers', *Polímeros*, vol. 25, no. 1, pp. 42–48, 2015. doi:10.1590/0104-1428.1495

[38] L. M. Pereira, A. C. Corrêa, M. de F. Rosa, and E. N. Ito, 'Rheological, morphological and mechanical characterization of recycled poly (ethylene terephthalate) blends and composites', *Mater. Res.*, vol. 20, no. 3, pp. 791–800, 2017. doi: 10.1590/1980-5373-mr-2016-0870

[39] M. Taşdemir and H. Ö. Gülsoy, 'Physical and mechanical properties of iron powder filled polystyrene composites', *Polym.-Plast. Technol. Eng.*, vol. 45, no. 11, pp. 1207–1211, 2006. doi:10.1080/03602550600887368

[40] L. S. Montagna and R. M. C. Santana, 'Influence of rubber particle size on properties of recycled thermoplastics containing rubber tyre waste', *Plast. Rubber Compos.*, vol. 41, no. 6, pp. 256–262, 2012. doi:10.1179/1743289811Y.0000000032

[41] W. K. Chee, N. A. Ibrahim, N. Zainuddin, M. F. Abd Rahman, and B. W. Chieng, 'Impact toughness and ductility enhancement of biodegradable poly (lactic acid)/poly (ε-caprolactone) blends via addition of glycidyl methacrylate', *Adv. Mater. Sci. Eng.*, vol. 2013, 2013.doi: 10.1155/2013/976373

[42] A. Gregorova, R. Wimmer, M. Hrabalova, M. Koller, T. Ters, and N. Mundigler, 'Effect of surface modification of beech wood flour on mechanical and thermal properties of poly (3-hydroxybutyrate)/wood flour composites', *Holzforschung*, vol. 63, no. 5, pp. 565–570, 2009. doi:10.1515/HF.2009.098

[43] M. Farhoodi *et al.*, 'Influence of TiO 2 nanoparticle filler on the properties of PET and PLA nanocomposites', *Polym. Korea*, vol. 36, no. 6, pp. 745–755, 2012. doi:10.7317/pk.2012.36.6.745

[44] J. Holbery and D. Houston, 'Natural-fiber-reinforced polymer composites in automotive applications', *Jom*, vol. 58, no. 11, pp. 80–86, 2006. doi: 10.1007/ s11837-006-0234-2

[45] P. Penjumras, R. AbdulRahman, R. A. Talib, and K. Abdan, ‘Effect of silanecoupling agent on properties of biocomposites based on poly (lactic acid) and durian rind cellulose’, 2016.

[46] M. E. Alemán-Domínguez, Z. Ortega, A. N. Benítez, G. Vilariño-Feltrer, J. A. Gómez-Tejedor, and A. Vallés-Lluch, ‘Tunability of polycaprolactone hydrophilicity by carboxymethyl cellulose loading’, *J. Appl. Polym. Sci.*, vol. 135, no. 14, p. 46134, 2018. doi: 10.1002/app.46134

[47] L. Wei, S. Liang, and A. G. McDonald, ‘Thermophysical properties and biodegradation behavior of green composites made from polyhydroxybutyrate and potato peel waste fermentation residue’, *Ind. Crops Prod.*, vol. 69, pp. 91–103, 2015. doi: 10.1016/j.indcrop.2015.02.011

[48] F. Awaja and D. Pavel, ‘Recycling of PET’, *Eur. Polym. J.*, vol. 41, no. 7, pp. 1453–1477, 2005. doi:10.1016/j.eurpolymj.2005.02.005

[49] M. M. Haafiz, A. Hassan, Z. Zakaria, I. M. Inuwa, M. S. Islam, and M. Jawaid, ‘Properties of polylactic acid composites reinforced with oil palm biomass microcrystalline cellulose’, *Carbohydr. Polym.*, vol. 98, no. 1, pp. 139–145, 2013. doi: 10.1016/j.carbpol.2013.05.069

[50] T. N. Tran *et al.*, ‘Cocoa shell waste biofilaments for 3D printing applications’, *Macromol. Mater. Eng.*, vol. 302, no. 11, p. 1700219, 2017. doi:10.1002/mame.201700219

[51] P. Dhar, U. Bhardwaj, A. Kumar, and V. Katiyar, ‘Poly (3-hydroxybutyrate)/ cellulose nanocrystal films for food packaging applications: Barrier and migration studies’, *Polym. Eng. Sci.*, vol. 55, no. 10, pp. 2388–2395, 2015. doi: 10.1002/pen.24127

[52] S. Nayak and S. kumar Khuntia, ‘Development and study of properties of Moringa oleifera fruit fibers/polyethylene terephthalate composites for packaging applications’, *Compos. Commun.*, vol. 15, pp. 113–119, 2019. doi: 10.1016/j.coco.2019.07.008

[53] A. S. Singha, R. K. Rana, and A. Rana, ‘Natural fiber reinforced polystyrene matrix based composites’, in *Advanced Materials Research*, 2010, vol. 123, pp. 1175–1178. doi: 10.4028/www.scientific.net/AMR.123-125.1175

[54] M. Milosevic, D. Stoof, and K. L. Pickering, ‘Characterizing the mechanical properties of fused deposition modelling natural fiber recycled polypropylene composites’, *J. Compos. Sci.*, vol. 1, no. 1, p. 7, 2017. doi: 10.3390/jcs1010007

[55] I. Navarro-Baena, V. Sessini, F. Dominici, L. Torre, J. M. Kenny, and L. Peponi, ‘Design of biodegradable blends based on PLA and PCL: From morphological, thermal and mechanical studies to shape memory behavior’, Polym. Degrad. Stab., vol. 132, pp. 97–108, 2016. doi:10.1016/j.polymdegradstab.2016.03.037

[56] S. Xie, ‘Plastics extrusion machine – SuThai plastic extrusion machinery’. https://suthaimachine.com/2016/10/25/nulla-metus-metus-ullamcorper-vel-tincidunt/ (accessed Dec. 25, 2020).

[57] R. Svečko, D. Kusić, T. Kek, A. Sarjaš, A. Hančič, and J. Grum, ‘Acoustic emission detection of macro-cracks on engraving tool steel inserts during the injection molding cycle using PZT sensors’, *Sensors*, vol. 13, no. 5, pp. 6365–6379, 2013. doi:10.3390/s130506365

[58] N. Saba, M. Jawaid, M. T. Paridah, and O. Y. Al-Othman, ‘A review on flammability of epoxy polymer, cellulosic and non-cellulosic fiber reinforced epoxy composites’, *Polym. Adv. Technol.*, vol. 27, no. 5, pp. 577–590, 2016. doi: 10.1002/pat.3739

[59] E. P. Cordeiro, V. J. Pita, and B. G. Soares, ‘Epoxy–fiber of peach palm trees composites: the effect of composition and fiber modification on mechanical and dynamic mechanical properties’, *J. Polym. Environ.*, vol. 25, no. 3, pp. 913–924, 2017. doi:10.1007/s10924-016-0841-0

[60] E. Rojo, M. V. Alonso, M. Oliet, B. Del Saz-Orozco, and F. Rodriguez, ‘Effect of fiber loading on the properties of treated cellulose fiber-reinforced phenolic composites’, *Compos. Part B Eng.*, vol. 68, pp. 185–192, 2015. doi:10.1016/j.compositesb.2014.08.047

[61] H. Kaddami *et al.*, ‘Short palm tree fibers–Thermoset matrices composites’, *Compos. Part Appl. Sci. Manuf.*, vol. 37, no. 9, pp. 1413–1422, 2006. doi:10.1016/j.compositesa.2005.06.020

[62] T. Lampke, S. Mishra, and A. Bismarck, ‘Plant fibers as reinforcement for green composites’, in *Natural fibers, biopolymers, and biocomposites*, CRC Press, 2005, pp. 52–128. doi:10.1201/9780203508206.ch2

[63] S. Taj, M. A. Munawar, and S. Khan, ‘Natural fiber-reinforced polymer composites’, *Proc.-Pak. Acad. Sci.*, vol. 44, no. 2, pp. 129–144, 2007.

[64] P. McKendry, ‘Energy production from biomass (part 1): overview of biomass’, *Bioresour. Technol.*, vol. 83, no. 1, pp. 37–46, 2002. doi: 10.1016/ s0960-8524(01)00118-3

[65] H. Yang, R. Yan, H. Chen, D. H. Lee, and C. Zheng, ‘Characteristics of hemicellulose, cellulose and lignin pyrolysis’, *Fuel*, vol. 86, no. 12–13, pp. 1781–1788, 2007. doi: 10.1016/j.fuel.2006.12.013

[66] G. T. Pott, ‘Natural fibers with low moisture sensitivity’, in *Natural fibers, plastics and composites*, Springer, 2004, pp. 105–122. doi: 10.1007/978-1-4419-9050-1_8

[67] A. Oushabi, S. Sair, F. O. Hassani, Y. Abboud, O. Tanane, and A. El Bouari, 'The effect of alkali treatment on mechanical, morphological and thermal properties of date palm fibers (DPFs): Study of the interface of DPF–Polyurethane composite', *South Afr. J. Chem. Eng.*, vol. 23, pp. 116–123, 2017. doi: 10.1016/j.sajce.2017.04.005

[68] I. Burgert, 'Exploring the micromechanical design of plant cell walls', *Am. J. Bot.*, vol. 93, no. 10, pp. 1391–1401, 2006. doi: 10.3732/ajb.93.10.1391

[69] F. M. Al-Oqla, M. T. Hayajneh, and O. Fares, 'Investigating the mechanical thermal and polymer interfacial characteristics of Jordanian lignocellulosic fibers to demonstrate their capabilities for sustainable green materials', *J. Clean. Prod.*, vol. 241, p. 118256, 2019. doi: 10.1016/j.jclepro.2019.118256

[70] L. Y. Mwaikambo and M. P. Ansell, 'Chemical modification of hemp, sisal, jute, and kapok fibers by alkalization', *J. Appl. Polym. Sci.*, vol. 84, no. 12, pp. 2222–2234, 2002. doi: 10.1002/app.10460

[71] S. V. Prasad, C. Pavithran, and P. K. Rohatgi, 'Alkali treatment of coir fibres for coir-polyester composites', *J. Mater. Sci.*, vol. 18, no. 5, pp. 1443–1454, 1983. doi:10.1007/bf01111964

[72] M. Poletto, A. J. Zattera, M. M. Forte, and R. M. Santana, 'Thermal decomposition of wood: Influence of wood components and cellulose crystallite size', *Bioresour. Technol.*, vol. 109, pp. 148–153, 2012. doi:10.1016/j.biortech.2011.11.122

[73] V. Tserki, P. Matzinos, S. Kokkou, and C. Panayiotou, 'Novel biodegradable composites based on treated lignocellulosic waste flour as filler. Part I. Surface chemical modification and characterization of waste flour', *Compos. Part Appl. Sci. Manuf.*, vol. 36, no. 7, pp. 965–974, 2005. doi: 10.1016/j.compositesa.2004.11.010

[74] J. Gassan and A. K. Bledzki, 'Thermal degradation of flax and jute fibers', *J. Appl. Polym. Sci.*, vol. 82, no. 6, pp. 1417–1422, 2001. doi:10.1002/app.1979

[75] H. L. Ornaghi, M. Poletto, A. J. Zattera, and S. C. Amico, 'Correlation of the thermal stability and the decomposition kinetics of six different vegetal fibers', *Cellulose*, vol. 21, no. 1, pp. 177–188, 2014. doi:10.1007/s10570-013-0094-1

[76] E. Gümüskaya, M. Usta, and H. Kirci, 'The effects of various pulping conditions on crystalline structure of cellulose in cotton linters', *Polym. Degrad. Stab.*, vol. 81, no. 3, pp. 559–564, 2003. doi: 10.1016/s0141-3910(03)00157-5

[77] K. Lau, P. Hung, M.-H. Zhu, and D. Hui, 'Properties of natural fibre composites for structural engineering applications', *Compos. Part B Eng.*, vol. 136, pp. 222–233, 2018. doi: 10.1016/j.compositesb.2017.10.038

[78] M. S. Lopes, A. L. Jardini, and R. Maciel Filho, ‘Poly (lactic acid) production for tissue engineering applications’, *Procedia Eng.*, vol. 42, pp. 1402–1413, 2012. doi: 10.1016/j.proeng.2012.07.534

[79] R. E. Drumright, P. R. Gruber, and D. E. Henton, ‘Polylactic acid technology’, *Adv. Mater.*, vol. 12, no. 23, pp. 1841–1846, 2000. doi: 10.1002/1521-4095(200012)12:23<1841::aid-adma1841>3.0.co;2-e

[80] L. W. McKeen, ‘Plastics used in medical devices’, in *Handbook of polymer applications in medicine and medical devices*, Elsevier, 2014, pp. 21–53. doi: 10.1016/b978-0-323-22805-3.00003-7

[81] M. Jamshidian, E. A. Tehrany, M. Imran, M. Jacquot, and S. Desobry, ‘Poly-lactic acid: production, applications, nanocomposites, and release studies’, *Compr. Rev. Food Sci. Food Saf.*, vol. 9, no. 5, pp. 552–571, 2010. doi: 10.1111/j.1541-4337.2010.00126.x

[82] A. J. Lasprilla, G. A. Martinez, B. H. Lunelli, A. L. Jardini, and R. Maciel Filho, ‘Poly-lactic acid synthesis for application in biomedical devices—A review’, *Biotechnol. Adv.*, vol. 30, no. 1, pp. 321–328, 2012. doi: 10.1016/j.biotechadv.2011.06.019

[83] R. L. Shogren, W. M. Doane, D. Garlotta, J. W. Lawton, and J. L. Willett, ‘Biodegradation of starch/polylactic acid/poly (hydroxyester-ether) composite bars in soil’, *Polym. Degrad. Stab.*, vol. 79, no. 3, pp. 405–411, 2003. doi: 10.1016/S0141-3910(02)00356-7

[84] D. J. Sawyer, ‘Bioprocessing–no longer a field of dreams’, in *Macromolecular symposia*, 2003, vol. 201, no. 1, pp. 271–282. doi: 10.1002/masy.200351130

[85] J. R. Dorgan, H. J. Lehermeier, L.-I. Palade, and J. Cicero, ‘Polylactides: properties and prospects of an environmentally benign plastic from renewable resources’, in *Macromolecular symposia*, 2001, vol. 175, no. 1, pp. 55–66. doi: 10.1002/1521-3900(200110)175:1<55::aid-masy55>3.0.co;2-k

[86] R. Auras, B. Harte, and S. Selke, ‘An overview of polylactides as packaging materials’, *Macromol. Biosci.*, vol. 4, no. 9, pp. 835–864, 2004. doi: 10.1002/mabi.200400043

[87] S. Jacobsen and H.-G. Fritz, ‘Plasticizing polylactide—the effect of different plasticizers on the mechanical properties’, *Polym. Eng. Sci.*, vol. 39, no. 7, pp. 1303–1310, 1999. doi: 10.1002/pen.11517

[88] M. Spinu, C. Jackson, M. Y. Keating, and K. H. Gardner, ‘Material design in poly (lactic acid) systems: block copolymers, star homo-and copolymers, and stereocomplexes’, *J. Macromol. Sci. Part Pure Appl. Chem.*, vol. 33, no. 10, pp. 1497–1530, 1996. doi: 10.1080/10601329608014922

[89] I. Pillin, N. Montrelay, A. Bourmaud, and Y. Grohens, ‘Effect of thermo-mechanical cycles on the physico-chemical properties of poly (lactic acid)’, *Polym. Degrad. Stab.*, vol. 93, no. 2, pp. 321–328, 2008. doi: 10.1016/j.polymdegradstab.2007.12.005

[90] H. Younes and D. Cohn, ‘Phase separation in poly (ethylene glycol)/poly (lactic acid) blends’, *Eur. Polym. J.*, vol. 24, no. 8, pp. 765–773, 1988. doi: 10.1016/0014-3057(88)90013-4

[91] M. Kumar, S. Mohanty, S. K. Nayak, and M. R. Parvaiz, ‘Effect of glycidyl methacrylate (GMA) on the thermal, mechanical and morphological property of biodegradable PLA/PBAT blend and its nanocomposites’, *Bioresour. Technol.*, vol. 101, no. 21, pp. 8406–8415, 2010. doi: 10.1016/j.biortech.2010.05.075

[92] L. Wang, W. Ma, R. A. Gross, and S. P. McCarthy, ‘Reactive compatibilization of biodegradable blends of poly (lactic acid) and poly (ε-caprolactone)’, *Polym. Degrad. Stab.*, vol. 59, no. 1–3, pp. 161–168, 1998. doi: 10.1016/s0141-3910(97)00196-1

[93] B. Ayana, S. Suin, and B. B. Khatua, ‘Highly exfoliated eco-friendly thermoplastic starch (TPS)/poly (lactic acid)(PLA)/clay nanocomposites using unmodified nanoclay’, *Carbohydr. Polym.*, vol. 110, pp. 430–439, 2014. doi: 10.1016/j.carbpol.2014.04.024

[94] Z. Ren, L. Dong, and Y. Yang, ‘Dynamic mechanical and thermal properties of plasticized poly (lactic acid)’, *J. Appl. Polym. Sci.*, vol. 101, no. 3, pp. 1583–1590, 2006. doi: 10.1002/app.23549

[95] M. Maiza, M. T. Benaniba, G. Quintard, and V. Massardier-Nageotte, ‘Biobased additive plasticizing Polylactic acid (PLA)’, *Polimeros*, vol. 25, no. 6, pp. 581–590, 2015. doi: 10.1590/0104-1428.1986

[96] V. Mazzanti, R. Pariante, A. Bonanno, O. R. de Ballesteros, F. Mollica, and G. Filippone, ‘Reinforcing mechanisms of natural fibers in green composites: Role of fibers morphology in a PLA/hemp model system’, *Compos. Sci. Technol.*, vol. 180, pp. 51–59, 2019. doi: 10.1016/j.compscitech.2019.05.015

[97] A. Awal, M. Rana, and M. Sain, ‘Thermorheological and mechanical properties of cellulose reinforced PLA bio-composites’, *Mech. Mater.*, vol. 80, pp. 87–95, 2015. doi: 10.1016/j.mechmat.2014.09.009

[98] W. Nuthong, P. Uawongsuwan, W. Pivsa-Art, and H. Hamada, ‘Impact property of flexible epoxy treated natural fiber reinforced PLA composites’, *Energy Procedia*, vol. 34, pp. 839–847, 2013. doi: 10.1016/j.egypro.2013.06.820

[99] M. Buchanan, ‘Solvent extractives of wood and pulp’. http://www.tappi.org/content/sarg/t204.pdf (accessed Dec. 25, 2020).

[100] M. Pracella, M. M.-U. Haque, and D. Puglia, ‘Morphology and properties tuning of PLA/cellulose nanocrystals bio-nanocomposites by means of reactive functionalization and blending with PVAc’, *Polymer*, vol. 55, no. 16, pp. 3720–3728, 2014. doi: 10.1016/j.polymer.2014.06.071

[101] S. F. Peaneus, ‘Estuaries.’ https://slideplayer.com/slide/12425387/ (accessed Dec. 25, 2020).

[102] M. J. M. Ridzuan, M. A. Majid, M. Afendi, M. N. Mazlee, and A. G. Gibson, ‘Thermal behaviour and dynamic mechanical analysis of Pennisetum purpureum/glass-reinforced epoxy hybrid composites’, *Compos. Struct.*, vol. 152, pp. 850–859, 2016. doi: 10.1016/j.compstruct.2016.06.026

[103] A. C. H. Barreto, M. A. Esmeraldo, D. S. Rosa, P. B. A. Fechine, and S. E. Mazzetto, ‘Cardanol biocomposites reinforced with jute fiber: microstructure, biodegradability, and mechanical properties’, *Polym. Compos.*, vol. 31, no. 11, pp. 1928–1937, 2010. doi: 10.1002/pc.20990

[104] E. H. Backes, L. de N. Pires, L. C. Costa, F. R. Passador, and L. A. Pessan, ‘Analysis of the degradation during melt processing of PLA/Biosilicate® composites’, *J. Compos. Sci.*, vol. 3, no. 2, p. 52, 2019. doi: 10.3390/jcs3020052

[105] N. Saba, M. T. Paridah, M. Jawaid, and O. Y. Alothman, ‘Thermal and flame retardancy behavior of oil palm based epoxy nanocomposites’, *J. Polym. Environ.*, vol. 26, no. 5, pp. 1844–1853, 2018. doi: 10.1007/s10924-017-1087-1

[106] H. Ibrahim, M. Farag, H. Megahed, and S. Mehanny, ‘Characteristics of starch-based biodegradable composites reinforced with date palm and flax fibers’, *Carbohydr. Polym.*, vol. 101, pp. 11–19, 2014. doi: 10.1016/j.carbpol.2013.08.051

[107] T. Khuenkeao, N. Petchwattana, and S. Covavisaruch, ‘Thermal and mechanical properties of bioplastic poly (lactic acid) compounded with silicone rubber and talc’, in *AIP Conference Proceedings- South Korea*, 2016, vol. 1713, no. 1, p. 080005.

[108] F. Tech, ‘Polymers and Plastics’, *Resources for Scientific Molding and Scientific Processing*. http://fimmtech.com/knowledgebase/polymers-and-plastics/ (accessed Dec. 25, 2020).

[109] E. Lezak, Z. Kulinski, R. Masirek, E. Piorkowska, M. Pracella, and K. Gadzinowska, ‘Mechanical and thermal properties of green polylactide composites with natural fillers’, *Macromol. Biosci.*, vol. 8, no. 12, pp. 1190–1200, 2008. doi: 10.1002/mabi.200800040

[110] K. Molnár, J. Móczó, M. Murariu, P. Dubois, and B. Pukánszky, 'Factors affecting the properties of PLA/CaSO4 composites: homogeneity and interactions', *EXPRESS Polym. Lett.*, vol. 3, pp. 49–61, 2009. doi: 10.3144/expresspolymlett.2009.8

[111] M. Kowalczyk, E. Piorkowska, P. Kulpinski, and M. Pracella, 'Mechanical and thermal properties of PLA composites with cellulose nanofibers and standard size fibers', *Compos. Part Appl. Sci. Manuf.*, vol. 42, no. 10, pp. 1509–1514, 2011. doi: 10.1016/j.compositesa.2011.07.003

[112] H. Boumediri, A. Bezazi, G. G. Del Pino, A. Haddad, F. Scarpa, and A. Dufresne, 'Extraction and characterization of vascular bundle and fiber strand from date palm rachis as potential bio-reinforcement in composite', *Carbohydr. Polym.*, vol. 222, p. 114997, 2019. doi: 10.1016/j.carbpol.2019.114997

[113] A. Bezazi, A. Belaadi, M. Bourchak, F. Scarpa, and K. Boba, 'Novel extraction techniques, chemical and mechanical characterisation of Agave americana L. natural fibres', *Compos. Part B Eng.*, vol. 66, pp. 194–203, 2014. doi: 10.1016/j.compositesb.2014.05.014

[114] M. Maache, A. Bezazi, S. Amroune, F. Scarpa, and A. Dufresne, 'Characterization of a novel natural cellulosic fiber from Juncus effusus L.', *Carbohydr. Polym.*, vol. 171, pp. 163–172, 2017. doi: 10.1016/j.carbpol.2017.04.096

[115] E. E. Popa *et al.*, 'Polylactic acid/cellulose fibres based composites for food packaging applications', *Mater Plast*, vol. 54, pp. 673–677, 2017. doi: 10.37358/Mat.Plast.1964

[116] J. P. Mofokeng, A. S. Luyt, T. Tábi, and J. Kovács, 'Comparison of injection moulded, natural fibre-reinforced composites with PP and PLA as matrices', *J. Thermoplast. Compos. Mater.*, vol. 25, no. 8, pp. 927–948, 2012. doi: 10.1177/0892705711423291

[117] M. T. Zafar, S. N. Maiti, and A. K. Ghosh, 'Effect of surface treatment of jute fibers on the interfacial adhesion in poly (lactic acid)/jute fiber biocomposites', *Fibers Polym.*, vol. 17, no. 2, pp. 266–274, 2016. doi: 10.1007/s12221-016-5781-8

[118] N. A. Rosli, I. Ahmad, F. H. Anuar, and I. Abdullah, 'Effectiveness of cellulosic Agave angustifolia fibres on the performance of compatibilised poly (lactic acid)-natural rubber blends', *Cellulose*, vol. 26, no. 5, pp. 3205–3218, 2019. doi: 10.1007/s10570-019-02262-x

[119] W. H. W. Ishak, N. A. Rosli, and I. Ahmad, 'Influence of amorphous cellulose on mechanical, thermal, and hydrolytic degradation of poly (lactic acid) biocomposites', *Sci. Rep.*, vol. 10, no. 1, pp. 1–13, 2020. doi: 10.1038/s41598-020-68274-x

[120] T. Semba, K. Kitagawa, U. S. Ishiaku, and H. Hamada, 'The effect of crosslinking on the mechanical properties of polylactic acid/polycaprolactone blends', *J. Appl. Polym. Sci.*, vol. 101, no. 3, pp. 1816–1825, 2006. doi: 10.1002/app.23589

[121] A. P. Mathew, K. Oksman, and M. Sain, 'Mechanical properties of biodegradable composites from poly lactic acid (PLA) and microcrystalline cellulose (MCC)', *J. Appl. Polym. Sci.*, vol. 97, no. 5, pp. 2014–2025, 2005. doi:10.1002/app.21779

[122] C. Nyambo, A. K. Mohanty, and M. Misra, 'Polylactide-based renewable green composites from agricultural residues and their hybrids', *Biomacromolecules*, vol. 11, no. 6, pp. 1654–1660, 2010. doi:10.1021/bm1003114

[123] K. Sungsanit, N. Kao, S. N. Bhattacharya, and S. Pivsaart, 'Physical and rheological properties of plasticized linear and branched PLA', *Korea-Aust. Rheol. J.*, vol. 22, no. 3, pp. 187–195, 2010.

[124] M. Barczewski and O. Mysiukiewicz, 'Rheological and processing properties of Poly(lactic acid) composites filled with ground chestnut shell', *Polym. Korea*, vol. 42, no. 2, pp. 267–274, 2018. doi: 10.7317/pk.2018.42.2.267

[125] S. Farsetti, B. Cioni, and A. Lazzeri, 'Physico-mechanical properties of biodegradable rubber toughened polymers', in *Macromolecular Symposia*, 2011, vol. 301, no. 1, pp. 82–89. doi: 10.1002/masy.201150311

[126] N. Herrera, A. A. Singh, A. M. Salaberria, J. Labidi, A. P. Mathew, and K. Oksman, 'Triethyl citrate (TEC) as a dispersing aid in polylactic acid/chitin nanocomposites prepared via liquid-assisted extrusion', *Polymers*, vol. 9, no. 9, p. 406, 2017. doi:10.3390/polym9090406

[127] S. Singh, M. Patel, D. Schwendemann, M. Zaccone, S. Geng, and M. L. Maspoch, 'Effect of chitin nanocrystals on crystallization and properties of Poly (lactic acid)-based nanocomposites', *Polymers*, vol. 12, no. 3, p. 726, 2020. doi: 10.3390/polym12030726

[128] D. C. França *et al.*, 'Tailoring PBAT/PLA/babassu films for suitability of agriculture mulch application', *J. Nat. Fibers*, vol. 16, no. 7, pp. 933–943, 2019. doi: 10.1080/15440478.2018.1441092

[129] X. Zhao, F. R. Guerrero, J. Llorca, and D.-Y. Wang, 'New superefficiently flame-retardant bioplastic poly (lactic acid): flammability, thermal decomposition behavior, and tensile properties', *ACS Sustain. Chem. Eng.*, vol. 4, no. 1, pp. 202–209, 2016. doi:10.1021/acssuschemeng.5b00980

[130] J. Jian, Z. Xiangbin, and H. Xianbo, 'An overview on synthesis, properties and applications of poly (butylene-adipate-co-terephthalate)–PBAT', *Adv. Ind. Eng. Polym. Res.*, vol. 3, no. 1, pp. 19–26, 2020. doi: 10.1016/ j.aiepr.2020.01.001

[131] B. Coppola, N. Cappetti, L. Di Maio, P. Scarfato, and L. Incarnato, '3D printing of PLA/clay nanocomposites: Influence of printing temperature on printed samples properties', *Materials*, vol. 11, no. 10, p. 1947, 2018. doi: 10.3390/ma11101947

[132] P. H. Manepalli, 'Use of thermoplastic starch in poly (lactic acid)/poly (butylene adipate-co-terephthalate) based nanocomposites for bio-based food packaging', 2019. (Doctoral dissertation) from Kansas State University, Manhattan, Kansas, United States.

[133] Y. Deng, C. Yu, P. Wongwiwattana, and N. L. Thomas, 'Optimising ductility of poly (lactic acid)/poly (butylene adipate-co-terephthalate) blends through co-continuous phase morphology', *J. Polym. Environ.*, vol. 26, no. 9, pp. 3802–3816, 2018. doi: 10.1007/s10924-018-1256-x

[134] J.-F. Zhang and X. Sun, 'Physical characterization of coupled poly (lactic acid)/starch/maleic anhydride blends plasticized by acetyl triethyl citrate', *Macromol. Biosci.*, vol. 4, no. 11, pp. 1053–1060, 2004. doi: 10.1002/mabi.200400076

[135] I. S. M. Tawakkal, R. A. Talib, K. Abdan, and C. N. Ling, 'Mechanical and physical properties of kenaf-derived cellulose (KDC)-filled polylactic acid (PLA) composites', *BioResources*, vol. 7, no. 2, pp. 1643–1655, 2012. doi: 10.15376/biores.7.2.1643-1655

[136] L. Yan and N. Chouw, 'Effect of water, seawater and alkaline solution ageing on mechanical properties of flax fabric/epoxy composites used for civil engineering applications', *Constr. Build. Mater.*, vol. 99, pp. 118–127, 2015. doi: 10.1016/j.conbuildmat.2015.09.025

[137] S. MR and B. Yogesha, 'Study on water absorption behaviour of jute and kenaf fabric reinforced epoxy composites: hybridization effect of e-glass fabric', *Int. J. Compos. Mater.*, vol. 6, no. 2, pp. 55–62, 2016. doi: 10.5923/j.cmaterials.20160602.03

[138] Y.-X. Weng, L. Wang, M. Zhang, X.-L. Wang, and Y.-Z. Wang, 'Biodegradation behavior of P (3HB, 4HB)/PLA blends in real soil environments', *Polym. Test.*, vol. 32, no. 1, pp. 60–70, 2013. doi: 10.1016/j.polymertesting.2012.09.014